IN PLANE VIBRATION OF LAYERED RINGS ON PERIODIC RADIAL SUPPORTS USING FINITE ELEMENT METHOD

by

J. V. SASTRY

DEPARTMENT OF MECHANICAL ENGINEERING

INDIAN INSTITUTE OF TECHNOLOGY KANPUR

JULY, 1986

IN PLANE VIBRATION OF LAYERED RINGS ON PERIODIC RADIAL SUPPORTS USING FINITE ELEMENT METHOD

A Thesis Submitted

In Partial Fulfilment of the Requirements

for the Degree of

MASTER OF TECHNOLOGY

by

J. V. SASTRY

to the

DEPARTMENT OF MECHANICAL ENGINEERING

INDIAN INSTITUTE OF TECHNOLOGY KANPUR

JULY, 1986

ME-1986-M-SAS-PLA

CERTIFICATE

This is to certify that the present work " IN PLANE VIBRATION OF LAYERED RINGS ON PERIODIC RADIAL SUPPORTS USING FINITE ELEMENT METHOD" has been carried out under our supervision and has not been submitted elsewhere for the award of a degree.

H. Hatwal
Asst. Professor
Mechanical Engg. Deptt.
I.I.T., Kanpur
INDIA

N.N. Kishore
Asst. Professor
Mechanical Engg. Deptt.
I.I.T., Kanpur
INDIA

July, 1986

ACKNOWLEDGEMENT

The author wishes to express his deep sense of gratitude and appreciation to his advisors Dr. N.N. Kishore and Dr. H. Hatwal who have guided this work from conception to completion.

The author would like to thank Dr. A.K. Mallik for the fruitful discussions during the period of this work which has helped in enlightening the author's ideas.

The author would like to thank all his friends, specially, Suresh, Subbarayudu, Baliga, Raghavan, Reddy and Gopinath for their timely help whenever necessary.

Thanks are also due to Mr. B.K. Jain for drawing the figures and to D.P. Saini, for producing the work in the present form.

CONTENTS

LIST OF FIGURES

LIST OF TABLES

LIST OF PRINCIPAL SYMBOLS

$\{ a^{(e)} \}$	Nodal displacement vector of the element.
$\{ a^{(c)} \}$	Nodal displacement vector of a complete bay of a ring.
$\{ a_L^{(c)} \}$	Nodal displacement vector of left hand boundary of a ring bay.
$\{ a_I^{(c)} \}$	Nodal displacement vector of intermediate nodes of one ring bay.
$\{ a_R^{(c)} \}$	Nodal displacement vector of right hand boundary of a ring bay.
b^r	Real part of eigenvector.
b^i	Imaginary part of eigenvector.
$[B]$	Strain displacement matrix of an element.
D_i	Bending stiffness of i^{th} layer $(= \frac{2}{3} E_i \, t \, \delta_i^3)$
$[D]$	Stress-strain matrix of a plane stress element of an isotropic material.
$[D_1]$, $[D_2]$	Stress-strain matrix of a plane stress orthotropic material.
E	Young's modulus of elasticity of an isotropic material.
E_L	Longitudinal Young's modulus.
E_T	Transverse Young's modulus.
E_i	Young's modulus of i^{th} layer of an isotropic material.

$\{ F \}$	Generalised force vector of one bay of the ring.
F_L , F_I , F_R	Generalised force vectors corresponding to left, intermediate and right nodes of a bay of a ring.
G_{TL}	Shear modulus of an orthotropic material.
h_i	Half thickness of i^{th} layer of the ring.
$[K^{(e)}]$	Element stiffness matrix.
$[K^{(c)}]$	Stiffness matrix for one complete bay of a ring.
K_r	Rotational stiffness.
$\bar{K}_r$	Nondimensional rotational stiffness $(K_r/D_2R_2^2)$.
K^r	Real part of the complex stiffness matrix
K^i	Imaginary part of the complex stiffness matrix.
$[M^{(c)}]$	Mass matrix of one complete bay of the ring.
$[M^{(e)}]$	Element mass matrix
M^r	Real part of complex mass matrix.
M^i	Imaginary part of complex mass matrix.
m_i	Mass of i^{th} layer $(=2\ t\ h_i\ \rho_i\ R_i)$.
n	Number of nodes in each bay of the ring.
NE	Number of elements in each bay of the ring
[N]	Shape function matrix.
N_i	Shape functions (i = 1....8)
Q_{ii}	Elements of the $[D_1]$ matrix.
R_i	Mid plane radius of i^{th} layer.
r	Radial coordinate of a point in an element.
r_i	Radial coordinate of nodes (i = 1....8)
s_i , t_i	Natural coordinates of element (i=1...8)
t	Width of the ring.

$[T_i]$	Transformation matrix of i^{th} element
T	Transpose of a matrix.
$\{u^{(e)}\}$	displacement vector of an element.
u	Radial displacement of a point in an element.
u_i	Radial displacement of nodes i = 1,2....8
v	Tangential displacement of a point in an element.
v_i	Tangential displacement of nodes i = 1,2...8
ω	Frequency.
α	Constant by which frequencies are shifted.
α_i	Gaussian quadrature weights.
δ_i	Ratio of half thickness to midplane radius (h_2/R_2) of i^{th} layer.
ρ_i	Density of i^{th} layer
ρ	Density of the material
μ_{rn}	Real part of propagation constant for n^{th} natural frequency.
μ_{in}	Imaginary part of propagation constant for n^{th} natural frequency.
μ	Propagation constant.
η	Phase difference between corresponding displacements of adjacent bays.
ϕ	Imaginary part of propagation constant.
θ	Angular coordinate of a point in an element.
θ_i	Angular coordinates of nodes i = 1,....8.

$\{\varepsilon^{(e)}\}^T$ Transpose of a strain vector.

ε_{rr} Principle strain.

$\varepsilon_{\theta\theta}$ Principle Strain.

$\varepsilon_{r\theta}$ Shear strain.

Ω_n Nondimensional n^{th} frequency $(=\sqrt{m_i/D_i})$ Nondimensionalising with respect to i^{th} layer properties.

ν Poisson's ratio

ν_{LT} Poisson ratio in L direction.

ν_{TL} Poisson ratio in T direction.

ν_{ZT} Poisson ratio in Z direction.

SYNOPSIS

IN PLANE VIBRATION OF LAYERED RINGS ON PERIODIC RADIAL SUPPORTS USING FINITE ELEMENT METHOD

A Thesis Submitted
In P artial Fulfilment of the Requirements
for the Degree of

MASTER OF TECHNOLOGY

by

J.V.SASTRY

to the

DEPARTMENT OF MECHANICAL ENGINEERING
INDIAN INSTITUTE OF TECHNOLOGY, KANPUR

JULY, 1986

The thesis presents the analysis of the in-plane vibration of layered rings with periodic supports using finite element approach.

Making use of wave propagation theory many researchers have found exact harmonic solutions to many problems. But the exact harmonic solution becomes very difficult to obtain, when anisotropy of the material is considered. In all such cases, th~ present FEM analysis would provide accurate propagation constants, natural frequencies and corresponding mode shapes.

In the present work, a finite element computer programme in FORTRAN-IV is developed and is implemented

on DEC-1090 system to get frequencies of a periodically supported beam and are found to compare well with the results presented by earlier workers.

The finite element approach is also used to get frequencies and mode shapes of a two layered elastic ring with the following support conditions,

Monocoupled

i) The supports prevent both radial and tangential displacements (u and v respectively) resulting in a monocoupled system having $\partial u/\partial\theta$ as the only coupling coordinate between one bay and next bay of the ring.

Bi-coupled

ii) The supports prevent only u, the radial displacement at the supports, thus making the system a Bi-coupled having v and $\partial u/\partial\theta$ as the coupling coordinates between one bay and the next bay of the ring and the natural frequencies are found to be within 0.5% accuracy compared to those presented by Reddy [9] who used wave approach.

Finally, the present method is applied to obtain frequencies and mode shapes of a three layered orthotropic ring and these results are tabulated.

CHAPTER - I

INTRODUCTION

1.1 Introduction and Literature Review:

Many structures like Bridges, Aircraft fuselage etc., contain a series of identical structural elements linked by identical junctions. These types of structures, with a regularly repeating section, having a combination of support conditions are referred to as periodic structures.

It is often required to study the dynamic behaviour of these structures for fluctuating pressure fields. Frequently it is also necessary to assess their vibration modes and response characteristics. Here it is interesting to note that, instead of finding the normal modes and natural frequencies of the structure, it is preferable to describe the behaviour of the periodic system by the properties of the characteristic waves, as this gives a better physical understanding of the system behaviour. Each of these characteristic waves is associated with a propagation constant. Also, there is a constant ratio between the amplitude of motion in one bay and that at the corresponding point

in the adjacent bay. The ratio of the amplitudes is equal to e^{μ}, where μ is the propagation constant, which may be in general a complex quantity. It's values always occur in positive and negative pairs corresponding to identical but opposite going waves. The real part of μ is known as 'Decay Constant' and the imaginary part is called the 'Phase Constant'.

Wave propagation will depend on whether for the particular wave, the propagation constant is purely real, purely imaginary or complex. If the propagation constant is purely real, the wave is non-propagating. In that case e^{μ} represents an exponential decay or growth of displacement from bay to bay, with corresponding displacements of adjacent bays being in phase. If propagation constant is purely imaginary (say $i\eta$) then the factor e^{μ} represents a simple phase difference of 'η' between the corresponding displacements of adjacent bays, but the amplitudes of the displacements are the same. If propagation constant μ has both non-zero real and imaginary parts, imaginary part being $\emptyset$, e^{μ} then represents exponential decay or growth of displacement but with corresponding displacements in adjacent bays being out of phase by an angle $\emptyset$.

Wave motion in simple periodic systems has been studied for nearly 300 years, as Brillouin [1]

electrical engineers have developed the studies over the years in relation to crystals, optics, electrical transmission lines, etc. Wave motion in engineering periodic structures (consisting of beams, plates etc.) has been investigated in early 70's. Heckl [2] considered a system of beams coupled together to form a regular grillage and demonstrated that waves propagate only in some frequency bands. Mead [3] included the effects of damping in the wave propagation theory for periodic beams and later, discussed the nature of the propagating waves and their possible interaction with acoustic waves [4].

In the literature referred to above, exact harmonic solutions have been found for the equations of motion of the periodic system. Mead [5] and Abrahamson [6] have discussed an extension of Rayleigh's method, and the Raleigh-Ritz technique, to permit a study of the propagating waves in non-uniform periodic structures. The significance of this is important, for it reveals the possibility of applying approximate methods, such as finite element technique, to wave propagation in periodic systems. Making use of finite element method Orris and Petyt [7] have considered two types of periodic construction, one a periodically supported infinite beam and the other a skin-rib

structure, to find the phase constants and then natural frequencies.

In the cases of the periodic structures made of anisotropic materials, it is quite difficult to get exact harmonic solution by analytical methods. In all such cases, finite element method can advantageously be used for finding the propagation constants and the natural frequencies. Mallick and Mead [8] analysed a periodically supported single layer ring analytically using wave propagation. Reddy [9] has analysed dynamic behaviour of layered rings on periodic supports by analytical approach. No material anisotropy has been considered in the above works.

In the present work, finite element approach has been applied to obtain natural frequencies and mode shapes of periodically supported beams and layered rings making use of wave propagation theory. The finite element program is developed to compare the natural frequencies of periodically supported beams obtained by Orris and Petyt [7]. Also it has been used to obtain the natural frequencies and mode shapes of two layered periodically supported ring with three supports and these have been compared with those presented by Reddy [9]. Finally layered orthotropic periodic ring on three supports has been considered and the natural

frequencies and mode shapes are obtained.

The work is broadly divided into three chapters. The second chapter deals with the finite element formulation of periodically supported layered ring to study the dynamic behaviour and the third chapter deals with the results and discussion. The results are presented for two layered radially supported ring. Both layers are considered elastic but of different materials. These are compared with the earlier results by Reddy [9]. Finally frequencies and mode shapes obtained by finite element program are presented for a layered orthotropic periodically supported ring.

CHAPTER - II

FINITE ELEMENT FORMULATION FOR PERIODIC RING STRUCTURE

2.1 Introduction:

Finite element method is a versatile numerical technique to analyze complicated structural problems. In recent years, it finds use in almost every engineering application. Analysis of vibration behaviour of structures is one such area where the technique has been extensively used to get accurate frequencies and mode shapes.

This chapter briefly outlines the theory of finite element formulation of periodically supported rings to find the propagation constants, natural frequencies and the associated mode shapes. Displacement formulation of the 8-node isoparametric element used in the present work is described.

Derivation of the eigen value problem expression for finding natural frequencies of a ring using finite element method and the method of solving the eigen value expression are described briefly. Finally, application of the method to the two layered ring with isotropic

material and three layered ring with orthotropic material, for finding frequencies and mode shapes is described.

2.2 Finite Element Formulation to Find the Propagation Constants and Frequencies of the Ring with Periodic Supports:

Finite element formulation applied to dynamic problems is described in several books [10-12]. In particular, the approach to find the propagation constants and frequencies of a periodic structure is described by Orris and Petyt [7]. The finite element formulation for ring type periodic structure follows a similar procedure which is described briefly in the following sections.

2.2.1 Finite Element Formulation by Displacement Method:

For the finite element displacement method of analysis of the periodically supported layered rings (Figs. 2.1 and 2.3), one bay of the ring structure is divided into an arbitrary number of discrete elements (Figs. 2.2 and 2.4). It may be noted that, bay is the span of the ring between one support and the next support. Within each element a polynomial type of expression is assumed for the displacement field. This displacement field is then related to the displacements at the nodal points located on the element boundaries.

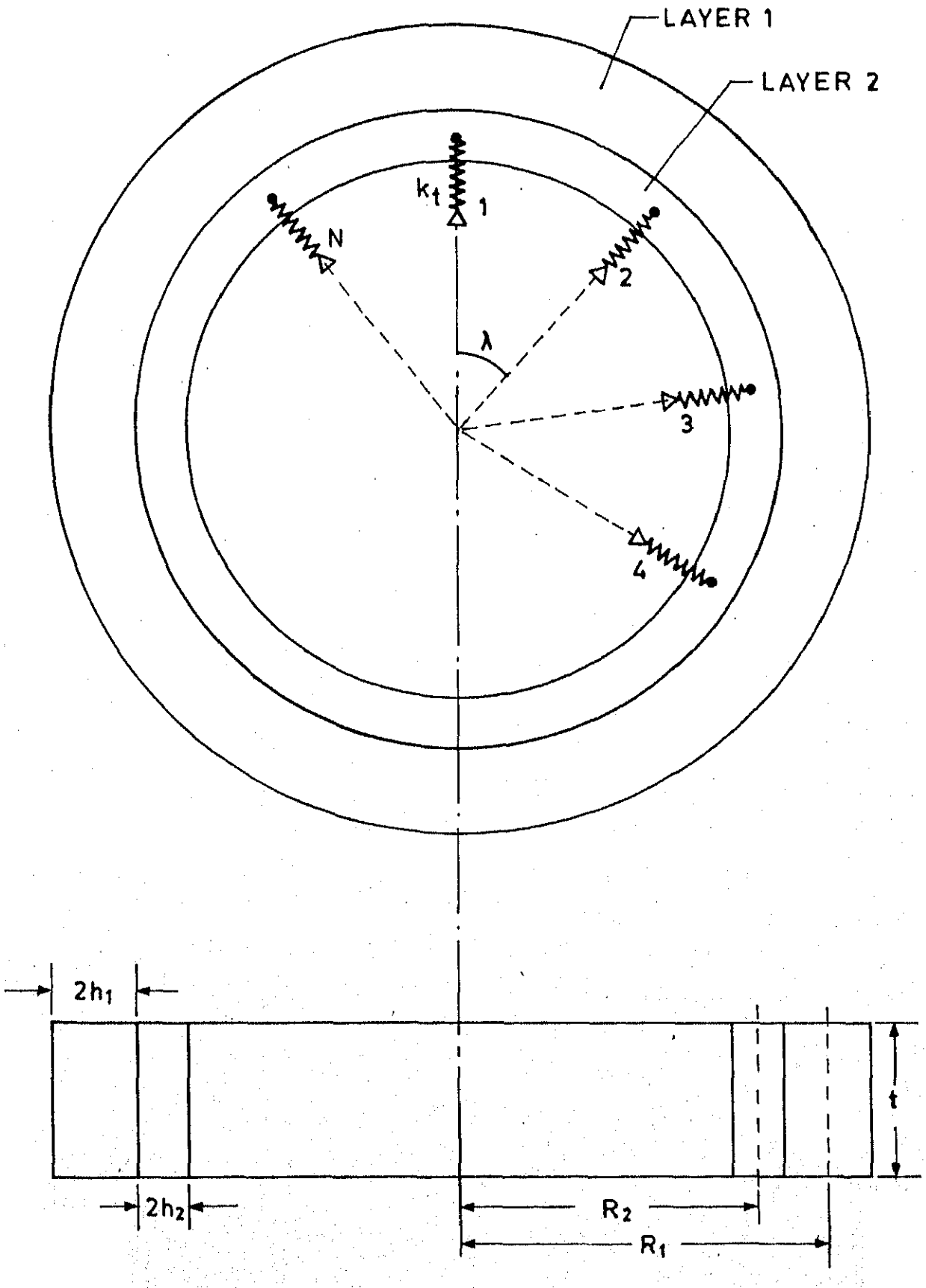

FIG. 2.1 TWO LAYERED RING ON EQUI-SPACED RADIAL SUPPORTS.

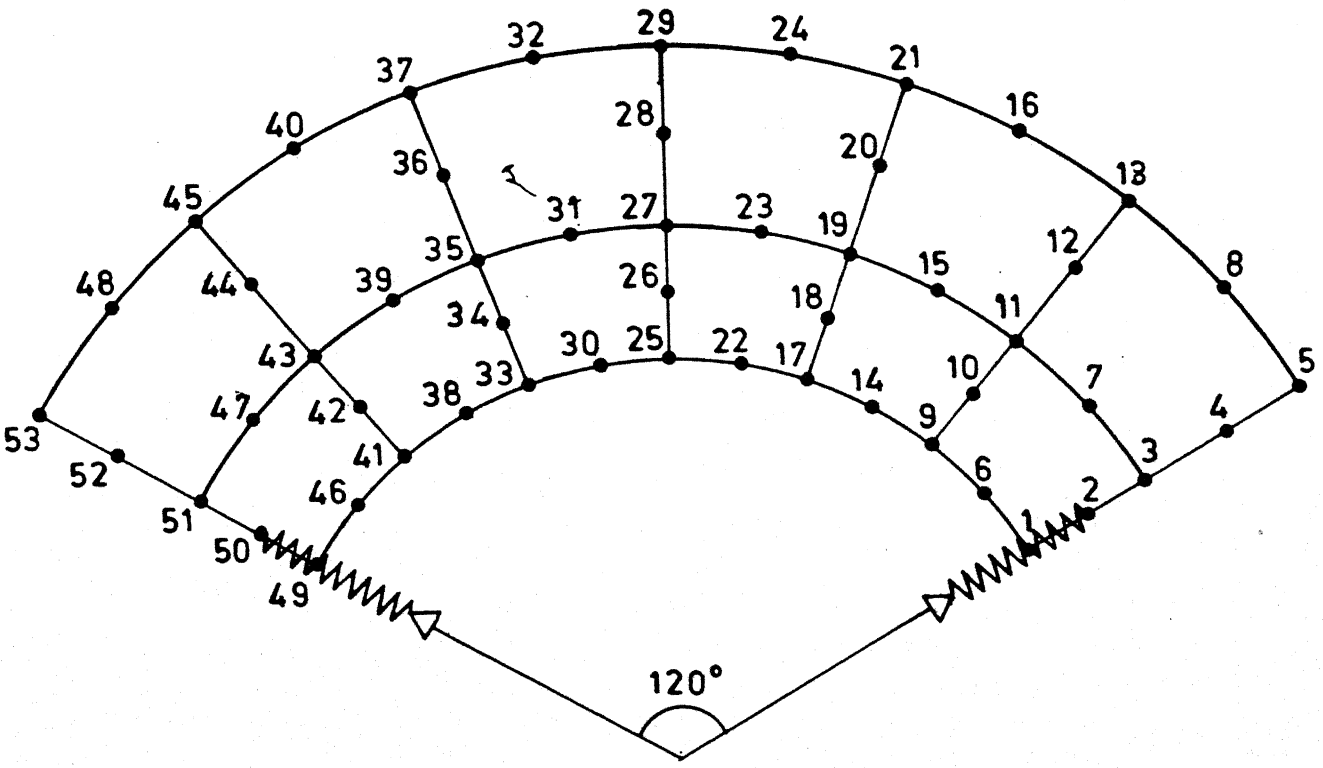

FIG. 2.2 PERIODIC BAY OF TWO LAYERED RING SHOWING FINITE ELEMENT MESH.

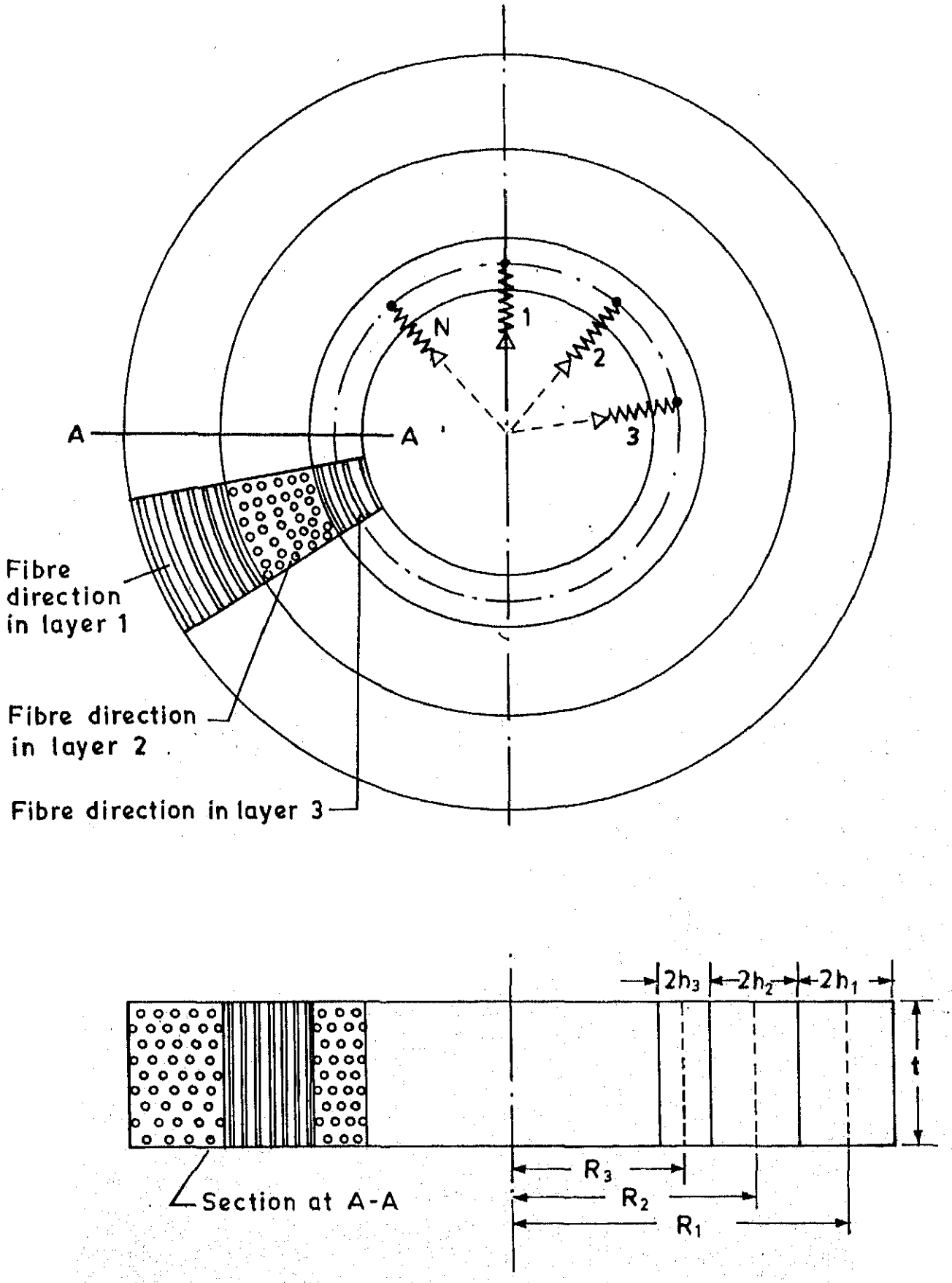

FIG. 2.3 THREE LAYRED ORTHOTROPIC RING.

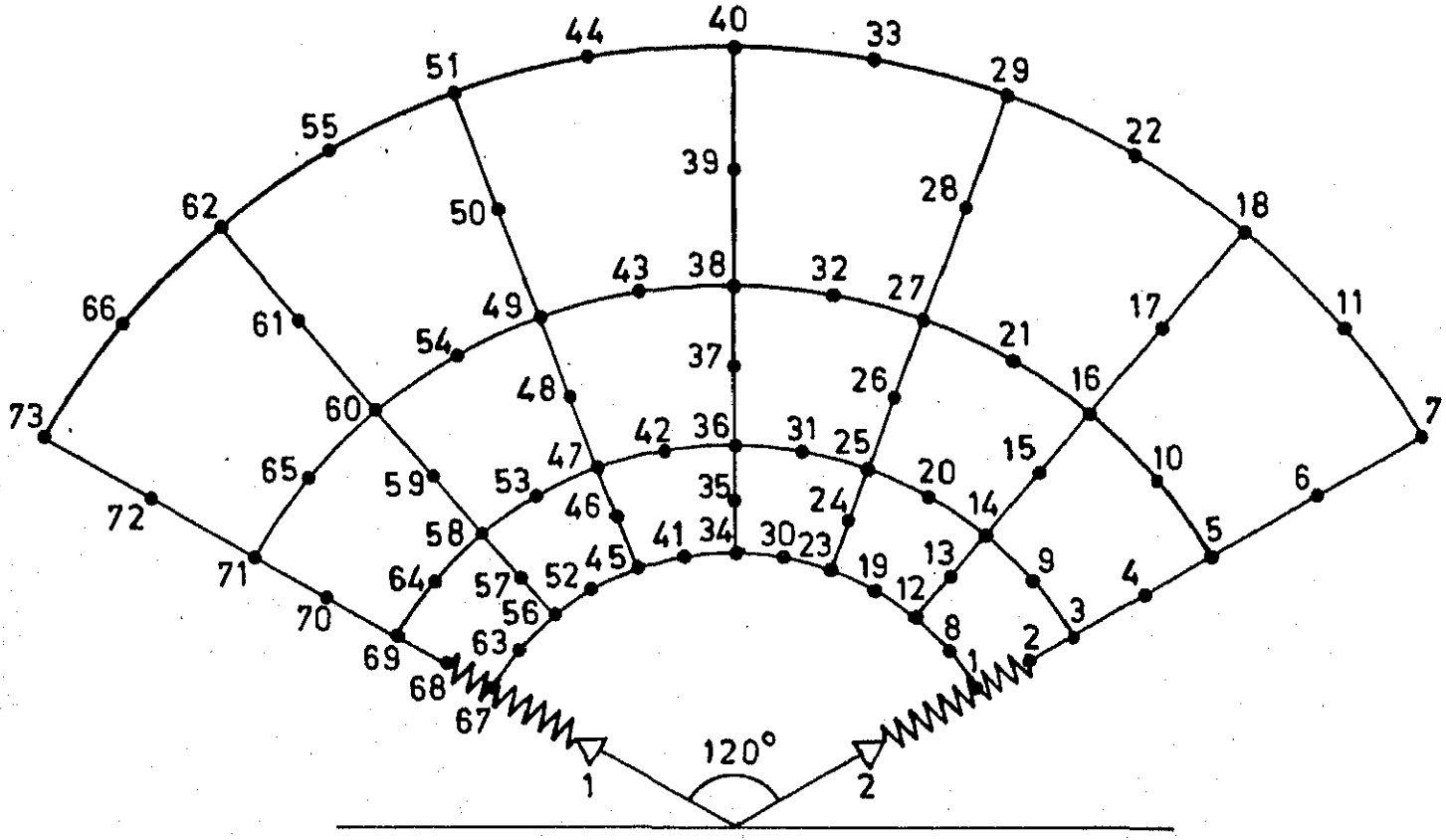

FIG.2.4 PERIODIC BAY OF A THREE LAYERED RING WITH FINITE ELEMENT MESH.

The development of the element stiffness and mass matrices is described in the following section.

2.2.2 Displacement Formulation of 8-node Isoparametric Element:

The unique description of the displacement within each element in terms of nodal values and boundary points or internal points of the element is the basic step in any displacement finite element formulation and can be expressed as

$$\{u\} = [N] \{a^{(e)}\} \qquad (2.1)$$

where $\{u\}$ is displacement vector.

$[N]$ is the shape function matrix

$\{a^{(e)}\}$ is the nodal displacement vector of the element.

If the shape functions chosen to describe the element geometry are identical to those used to prescribe function (displacement) variation, then the element is termed iso-parametric. A typical isoparametric element is shown in Fig. (2.5). The functional property of the interpolation function 'N_i' is that its value in the natural coordinate system is unity at node 'i' and zero at all other nodes. The formulation given below follows general pattern of derivation suggested by Bathe and Wilson [12] and Zienkiewicz [13]. For a two dimensional

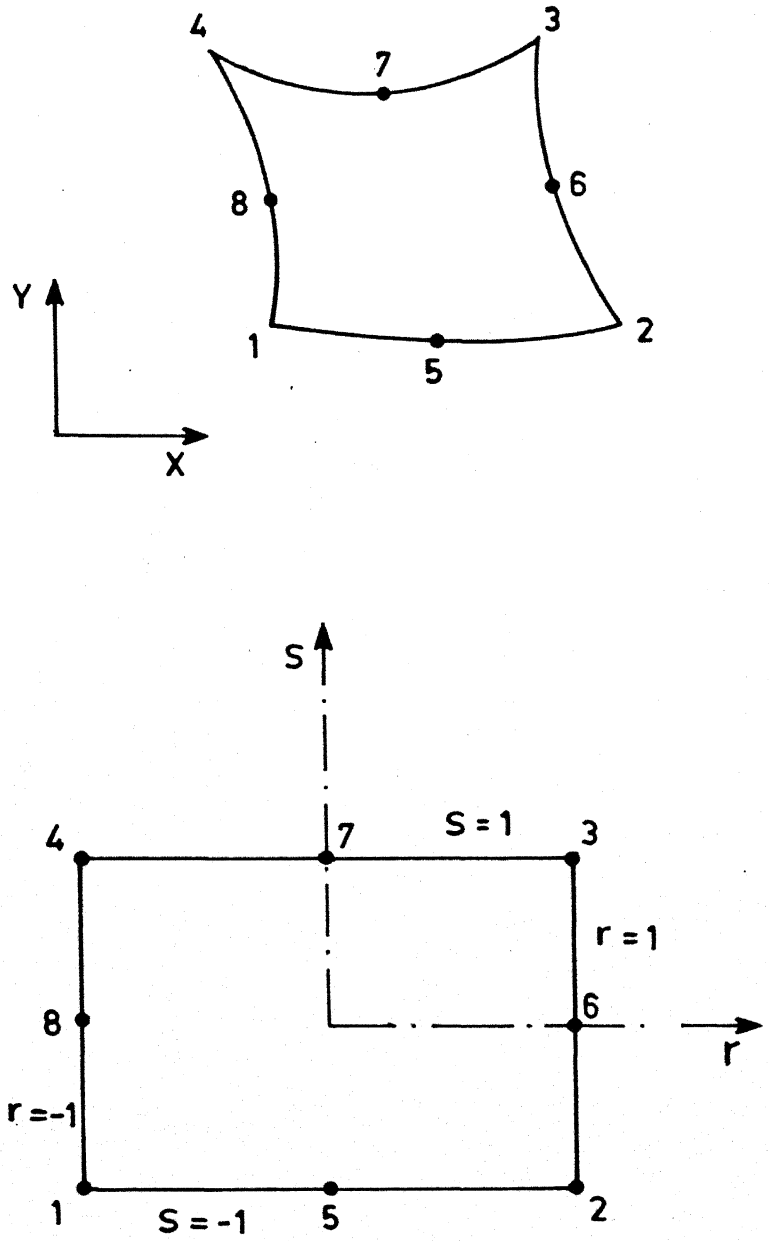

FIG. 2.5 ISOPARAMETRIC ELEMENT TRANSFORMATION FROM LOCAL TO GLOBAL COORDINATES.

8-node element, a quadratic variation of the displacement and geometry are assumed and interpolation functions N_1 to N_8 are given in Appendix A. Thus, it has 16 displacement degrees of freedom, two degrees of freedom being for each node. Polar coordinates r, θ and natural coordinates s_i , t_i are related as follows:

$$r = N_1 r_1 + N_2 r_2 + N_3 r_3 + N_4 r_4 + N_5 r_5 + N_6 r_6 + N_7 r_7 + N_8 r_8 \qquad (2.2a)$$

$$\theta = N_1 \theta_1 + N_2 \theta_2 + N_3 \theta_3 + N_4 \theta_4 + N_5 \theta_5 + N_6 \theta_6 + N_7 \theta_7 + N_8 \theta_8 \qquad (2.2b)$$

Similarly, the displacements expressed in nodal values are:

$$u = N_1 u_1 + N_2 u_2 + N_3 u_3 + N_4 u_4 + N_5 u_5 + N_6 u_6 + N_7 u_7 + N_8 u_8 \qquad (2.3a)$$

$$v = N_1 v_1 + N_2 v_2 + N_3 v_3 + N_4 v_4 + N_5 v_5 + N_6 v_6 + N_7 v_7 + N_8 v_8 \qquad (2.3b)$$

Thus, the above two equations may be written in matrix notation as

$$\{ u^{(e)} \} = [N] \{ a^{(e)} \} \qquad (2.4)$$

where $$\{ u^{(e)} \} = \begin{Bmatrix} u \\ v \end{Bmatrix} \qquad (2.4a)$$

$$[N] = \begin{bmatrix} N_1 & 0 & N_2 & 0 & N_3 & 0 & N_4 & 0 & N_5 & 0 & N_6 & 0 & N_7 & 0 & N_8 & 0 \\ 0 & N_1 & 0 & N_2 & 0 & N_3 & 0 & N_4 & 0 & N_5 & 0 & N_6 & 0 & N_7 & 0 & N_8 \end{bmatrix} \qquad (2.4b)$$

....

$$\{a^{(e)}\}^T = [u_1\ v_1\ u_2\ v_2\ u_3\ v_3\ u_4\ v_4\ u_5\ v_5\ u_6\ v_6\ u_7\ v_7\ u_8\ v_8] \qquad (2.4c)$$

The element strain vector for plane stress case is

$$\{\varepsilon^{(e)}\}^T = [\varepsilon_{rr}\ \ \varepsilon_{\theta\theta}\ \ \varepsilon_{r\theta}] \qquad (2.5a)$$

where,

$$\varepsilon_{rr} = \frac{\partial u}{\partial r},\ \varepsilon_{\theta\theta} = \frac{\partial v}{\partial \theta},\ \varepsilon_{r\theta} = \frac{\partial v}{\partial r} + \frac{\partial u}{\partial \theta} \qquad (2.5b)$$

The strains at any point within an element are related to the nodal displacements by

$$\{\varepsilon^{(e)}\} = [B]\ \{a^{(e)}\} \qquad (2.6a)$$

where strain displacement matrix is given by

$$[B] = \begin{bmatrix} \frac{\partial N_1}{\partial r} & 0 & \frac{\partial N_2}{\partial r} & 0 & \frac{\partial N_3}{\partial r} & 0 & \frac{\partial N_4}{\partial r} & 0 & \frac{\partial N_5}{\partial r} & 0 & \frac{\partial N_6}{\partial r} & 0 & \frac{\partial N_7}{\partial r} & 0 & \frac{\partial N_8}{\partial r} & 0 \\ 0 & \frac{\partial N_1}{\partial \theta} & 0 & \frac{\partial N_2}{\partial \theta} & 0 & \frac{\partial N_3}{\partial \theta} & 0 & \frac{\partial N_4}{\partial \theta} & 0 & \frac{\partial N_5}{\partial \theta} & 0 & \frac{\partial N_6}{\partial \theta} & 0 & \frac{\partial N_7}{\partial \theta} & 0 & \frac{\partial N_8}{\partial \theta} \\ \frac{\partial N_1}{\partial \theta} & \frac{\partial N_1}{\partial r} & \frac{\partial N_2}{\partial \theta} & \frac{\partial N_2}{\partial r} & \frac{\partial N_3}{\partial \theta} & \frac{\partial N_3}{\partial r} & \frac{\partial N_4}{\partial \theta} & \frac{\partial N_4}{\partial r} & \frac{\partial N_5}{\partial \theta} & \frac{\partial N_5}{\partial r} & \frac{\partial N_6}{\partial \theta} & \frac{\partial N_6}{\partial r} & \frac{\partial N_7}{\partial \theta} & \frac{\partial N_7}{\partial r} & \frac{\partial N_8}{\partial \theta} & \frac{\partial N_8}{\partial r} \end{bmatrix}$$

... (2.6b)

For plane stress, the elasticity (stress-strain) matrix for isotropic material can be written as

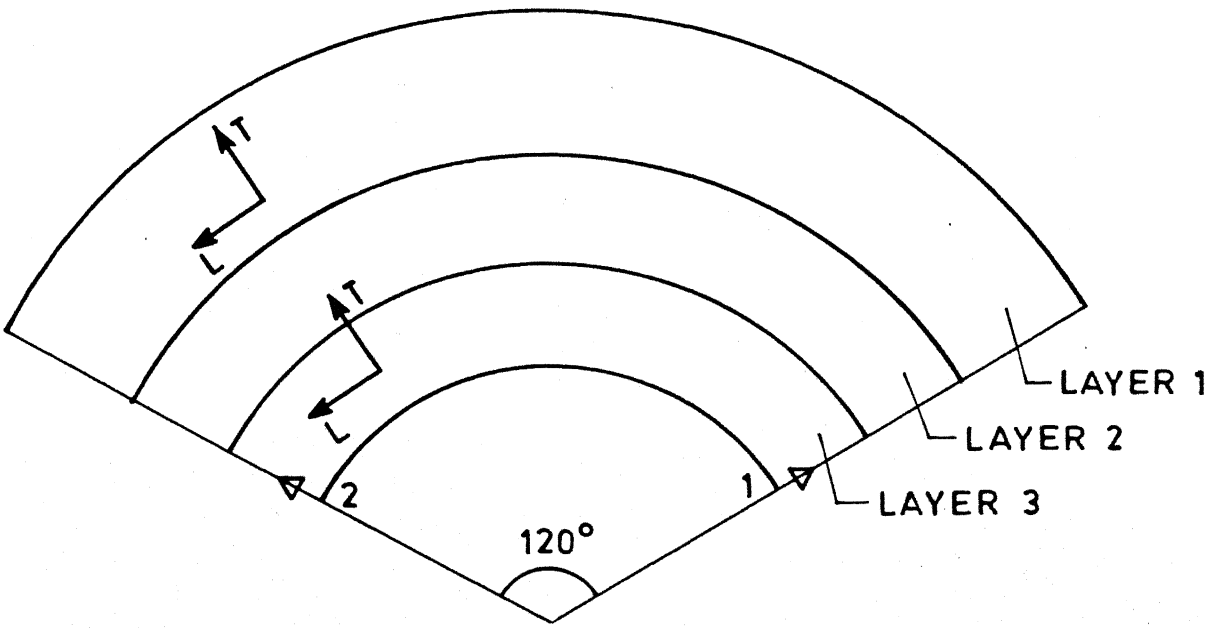

FIG. 2.6 LONGITUDINAL AND TRANSVERSE DIRECTIONS OF FIBRES IN LAYER 3 AND 1.

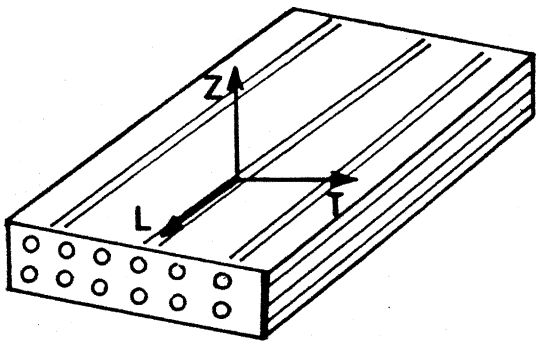

FIG. 2.7 MATERIAL AXIS L, T, Z FOR A LAMINA (ORTHOTROPIC LAYER)

$$[D] = \frac{E}{1-\nu^2} \begin{bmatrix} 1 & \nu & 0 \\ \nu & 1 & 0 \\ 0 & 0 & \frac{1-\nu}{2} \end{bmatrix} \qquad (2.7)$$

where 'E' is the Young's modulus of elasticity

ν is the Poisson's ratio

For orthotropic material, the stress-strain matrix for plane stress case when the fibres are oriented as shown in Fig. (2.6) can be written as

$$[D_1] = \begin{bmatrix} Q_{11} & Q_{12} & 0 \\ Q_{21} & Q_{22} & 0 \\ 0 & 0 & Q_{33} \end{bmatrix} \qquad (2.8)$$

where

$$Q_{11} = \frac{E_L}{1 - \nu_{LT}\,\nu_{TL}} \qquad (2.8a)$$

$$Q_{12} = \frac{\nu_{LT}\,E_T}{1 - \nu_{LT}\,\nu_{TL}} \qquad (2.8b)$$

$$Q_{21} = Q_{12} \qquad (2.8c)$$

$$Q_{22} = \frac{E_T}{1-\nu_{LT}\,\nu_{TL}} \qquad (2.8d)$$

$$Q_{33} = G_{LT} \qquad (2.8e)$$

E_L is the Young's modulus in the direction of fibre axis

E_T is the Young's modulus in the perpendicular direction of the fibre axis

G_{TL} is the shear modulus

ν_{LT} is the Poisson ratio in the direction of the fibre

ν_{TL} is the Poisson ratio in the direction transverse to the fibre axis

For orthotropic material, the stress-strain matrix for plane stress case when the fibres are oriented as shown in Fig. (2.7) can be written as

$$[D_2] = \frac{E_T}{1-\nu_{ZT}^2} \begin{bmatrix} 1 & \nu_{ZT} & 0 \\ \nu_{ZT} & 1 & 0 \\ 0 & 0 & \frac{1-\nu_{ZT}}{2} \end{bmatrix} \qquad (2.9)$$

where E_T is the Young's modulus in the perpendicular direction of fibre axis

and ν_{ZT} is the Poisson ratio in the Z direction Fig. (2.7a)

The stiffness matrix $K^{(e)}$ and mass matrix $M^{(e)}$ of the element can be evaluated as

$$K^{(e)} = \int B^T D B \, dV \qquad (2.10)$$

$$M^{(e)} = \int \rho N^T N \, dV \qquad (2.11)$$

where 'ρ' is density of the material of the element.

The matrices in general are evaluated by numerical integration, using Gaussian quadrature formula. For plane stress condition, thickness 't' being constant, the matrices $K^{(e)}$ and $M^{(e)}$ can be obtained as

$$K^{(e)} = t \sum_{i=1}^{n} \sum_{j=1}^{n} \alpha_i \alpha_j F_{ij} \qquad (2.12a)$$

where $$F_{ij} = B_{ij}^T D B_{ij} r_{ij} \text{ Det } J_{ij} \qquad (2.12b)$$

and

$$M^{(e)} = t \sum_{i=1}^{n} \sum_{j=1}^{n} \alpha_i \alpha_j F'_{ij} \qquad (2.13a)$$

where $$F'_{ij} = \rho [N_{ij}]^T [N_{ij}] r_{ij} \text{ Det } . J_{ij} \qquad (2.13b)$$

In the above equations, 'r_{ij}' is the radial coordinate of i^{th} Gaussian point, and n are the number of integration points in each coordinate direction, Det.J_{ij} is the determinant of the Jacobian matrix of transformation.

α_i are Gaussian quadrature weights of the i^{th} Gaussian point.

F_{ij} , F'_{ij} are function values to be evaluated at Gaussian points S_i , t_i

For evaluation of the stiffness matrix of the element, a 2 x 2 numerical integration is used. For the evaluation of the mass matrix of the element, a 4 x 4 integration order leading to the summation of functions evaluated at 16 sampling points is used.

2.2.3 Development of Assembled Stiffness and Mass Matrices of the Structure:

The assembly of the stiffness and mass matrices of all the elements is carried out to get the complete

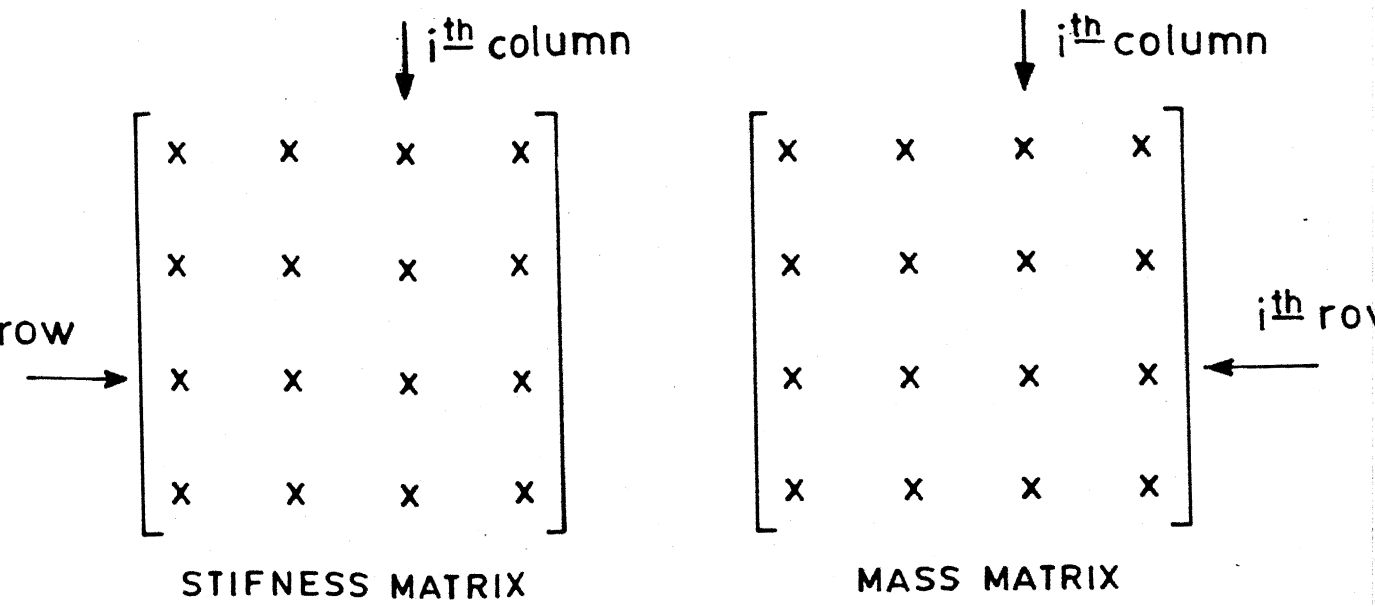

BEFORE APPLYING BOUNDARY CONDITIONS

$$\begin{bmatrix} x & x & 0 & x \\ x & x & 0 & x \\ 0 & 0 & 10^{-9} & 0 \\ x & x & 0 & x \end{bmatrix} \qquad \begin{bmatrix} x & x & 0 & x \\ x & x & 0 & x \\ 0 & 0 & 1 & 0 \\ x & x & 0 & x \end{bmatrix}$$

STIFFNESS MATRIX MASS MATRIX

AFTER APPLYING BOUNDARY CONDITIONS

FIG. 2.8 APPLYING BOUNDARY CONDITIONS FOR STIFNESS AND MASS MATRICES.

stiffness and mass matrices of one bay of the ring. If the vector of nodal displacements for the complete ring is $\{a^c\}$, then the nodal displacements vector of an individual element $\{a_i^{(e)}\}$ is related by a transformation matrix $[T_i]$ given by

$$\{a_i^{(e)}\} = [T_i] \{a^c\} \tag{2.14}$$

where

$$\{a^c\} = \begin{bmatrix} r_1 \\ \theta_1 \\ r_2 \\ \theta_2 \\ \vdots \\ r_n \\ \theta_n \end{bmatrix} \tag{2.14a}$$

where 'n' indicates total number of nodes for one bay of the ring.

The stiffness matrix for one complete bay of the ring consisting of 'NE' elements is then given by

$$[K^c] = \sum_{i=1}^{NE} [T_i]^T [K_i^{(e)}] [T_i] \tag{2.15}$$

A similar expression gives the mass matrix $[M^c]$ of one complete bay of the ring.

2.2.4 Boundary Conditions:

After the assembly of stiffness and mass matrices, displacement boundary conditions are imposed on them, thus making them non-singular. In this section, the application of different boundary conditions for one bay of a two layered and a three layered ring are described. There are different ways of imposing the boundary conditions. The method used in the present work is described as follows.

Consider i^{th} degree of freedom to be constrained. The procedure is to make all elements of the stiffness and mass matrices corresponding to i^{th} row and column as zeros except the diagonal element of i^{th} row. This diagonal element in the present case is chosen to be sufficiently high and corresponding element in the mass matrix is made unity. This ensures, a unit eigen value corresponding to i^{th} degree of freedom to be eliminated in finding fundamental frequencies by subspace iteration technique of solving eigen value problem.

The boundary conditions for monocoupled system are applied to the node on the support boundary at mid-plane radius. Both the radial and tangential degrees of freedom are constrained.

For Bicoupled case, only radial degree of freedom is constrained at the node on the boundary lying on midplane radius of base layer 2.

For a three layered monocoupled system, the boundary conditions are applied in a similar manner, only difference being that, the node on the boundaries on the midplane radius of base layer 3 are considered instead of base layer 2 as in the case of monocoupled case.

2.2.5 Formulation of Eigen Value Expression for Propagation Constants and Eigen Values:

Considering the periodic ring structure shown schematically Fig. (2.9), each periodic component AA'BB', could be described by an identical arrangement of elements. These periodically occurring element grids are connected by the displacements on the boundaries AA', BB',

The assembled vector of nodal displacements for one of the sections, AA'BB' will contain degrees of freedom corresponding to nodes on the left hand boundary $\{a_L^c\}$, the right hand boundary $\{a_R^c\}$, and all other nodes, $\{a_I^c\}$. Thus, the vector of nodal displacements for the section after the application of constraints is

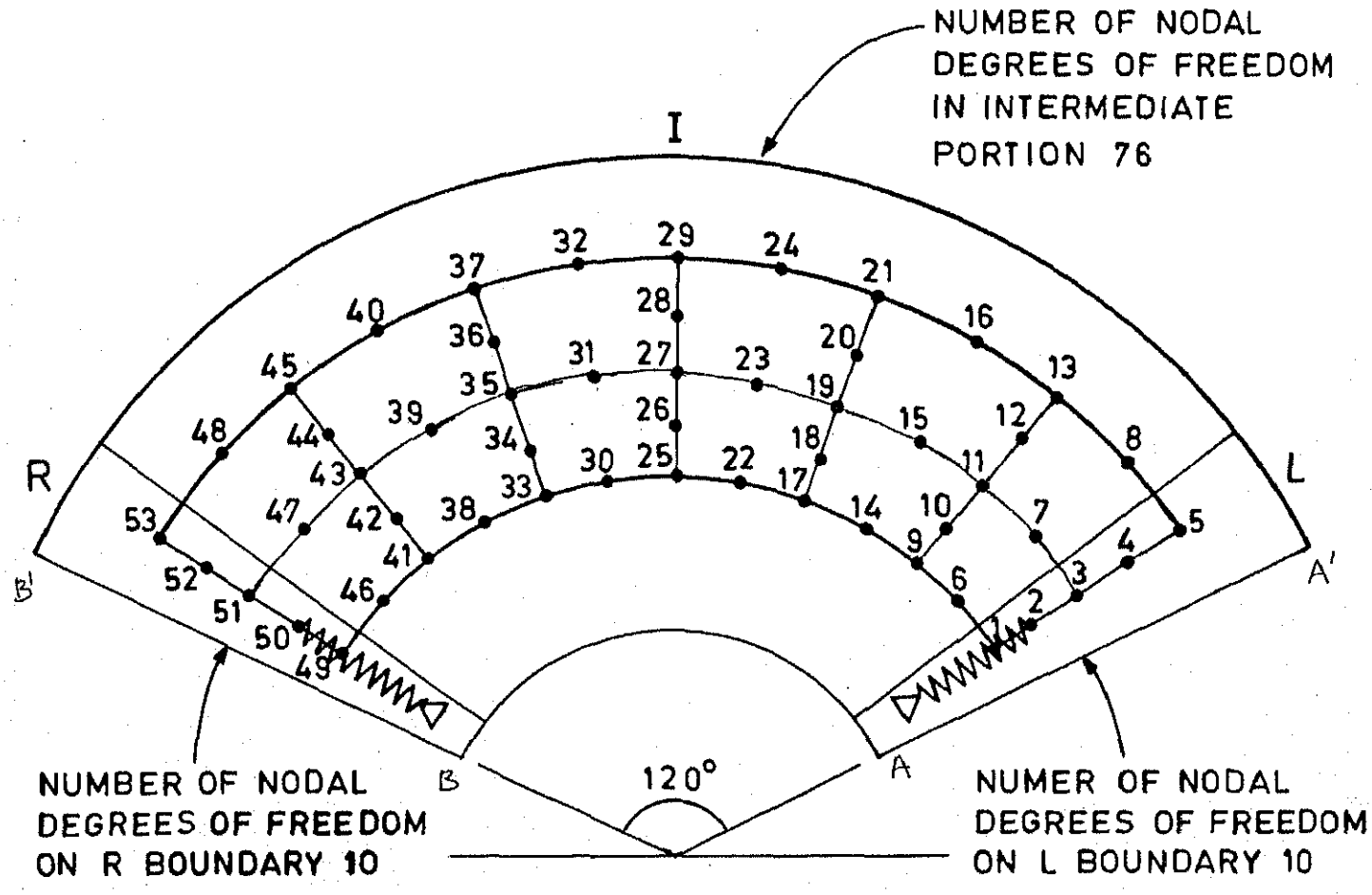

FIG.2.9 LOCATION OF NODES ON L AND R BOUNDARIES.

$$\{a^c\} = \begin{bmatrix} a_L^{(c)} \\ a_I^{(c)} \\ a_R^{(c)} \end{bmatrix} \qquad (2.16)$$

Corresponding to each nodal displacement, this will be a generalised force. The force vector for the periodic section may be defined as

$$\{F\} = \begin{bmatrix} F_L \\ F_I \\ F_R \end{bmatrix} \qquad (2.17)$$

When the periodic system vibrates harmonically with angular frequency ω, the equation of motion is

$$([K^{(c)}] - \omega^2 [M^{(c)}]) \{a^{(c)}\} = \{F\} \qquad (2.18)$$

where $[K^{(c)}]$ and $[M^{(c)}]$ are defined with equation (2.15), $\{a^{(c)}\}$ by equation (2.14a) and $\{F\}$ by equation (2.17).

At this stage, in order to facilitate the general solution of equation (2.18), the displacements $\{a^{(c)}\}$ and forces $\{F\}$ are allowed to take complex values.

When a free wave propagates through an infinite structure, $\{F_I\}$ is zero. The ratio between corresponding displacements in adjacent bays of the structure is equal to e^{μ}, where 'μ' is the complex propagation constant. The nodal forces at the exterior nodes of the section, $\{F_L\}$ and $\{F_R\}$, are not zero, since these

are internal forces in the over all structure.

The nodal displacements along the left hand boundary and those at the corresponding right hand boundary of the section are related by the propagation constant. Thus, if the node numbering sequence on the right hand boundary is identical to that on the left hand boundary, the nodal displacements are related by,

$$\{a_R^{(c)}\} = e^{\mu} \{a_L^{(c)}\} \qquad (2.19)$$

Similarly, it may be shown that for equilibrium between adjacent sections the nodal forces and moments at the left hand and right hand boundaries are related by,

$$\{F_R\} = - e^{\mu} \{F_L\} \qquad (2.20)$$

when equations (2.19) and (2.20) are substituted into equation (2.18), with $\{F_I\} = 0$, the equation of motion of the periodic section becomes

$$([K^{(c)}] - \omega^2 [M^{(c)}]) \begin{bmatrix} a_L^{(c)} \\ a_I^{(c)} \\ a_L^{(c)} \; e^{\mu} \end{bmatrix} = \begin{bmatrix} F_L \\ 0 \\ -e^{\mu} F_L \end{bmatrix} \qquad (2.21)$$

The assembled mass and stiffness matrices, $[K^c]$ and $[M^c]$, may be partitioned to correspond with the three types of nodes, those on the left hand boundary, those on the right hand boundary, and all other, interior, nodes. Thus,

$$[K^c] = \begin{bmatrix} K_{LL} & K_{LI} & K_{LR} \\ K_{IL} & K_{II} & K_{IR} \\ K_{RL} & K_{RI} & K_{RR} \end{bmatrix} \quad \text{and} \qquad (2.22)$$

$$[M^c] = \begin{bmatrix} M_{LL} & M_{LI} & M_{LR} \\ M_{IL} & M_{II} & M_{IR} \\ M_{RL} & M_{RI} & M_{RR} \end{bmatrix} \qquad (2.23)$$

Using the relation (2.19) and (2.20) the total number of degrees of freedom present for the constrained system (2.21) may now be reduced by the number of degrees of freedom along the right hand boundary of the section. The matrix equation then found is

$$\left[\begin{array}{cc|c} K_{LL} + K_{RR} + e^{\mu} K_{LR} + e^{-\mu} K_{RL} & & K_{LI} + e^{-\mu} K_{RI} \\ \hline K_{IL} + e^{\mu} K_{IR} & & K_{II} \end{array}\right] \begin{bmatrix} a_L^{(c)} \\ a_I^{(c)} \end{bmatrix}$$

$$-\omega^2 \left[\begin{array}{cc|c} M_{LL} + M_{RR} + e^{\mu} M_{LR} + e^{-\mu} M_{RL} & & M_{LI} + e^{-\mu} M_{RI} \\ \hline M_{IL} + e^{\mu} M_{IR} & & M_{II} \end{array}\right] \begin{bmatrix} a_L^{(c)} \\ a_I^{(c)} \end{bmatrix} = 0$$

$$\ldots \qquad (2.24)$$

or, in abbreviated form,

$$[K(\mu)] - \omega^2 [M(\mu)] \begin{bmatrix} a_L^{(c)} \\ a_I^{(c)} \end{bmatrix} = 0 \qquad (2.25)$$

where $[K(\mu)]$, $[M(\mu)]$ are real functions of the complex variable μ.

The set of equations (2.25) represent an eigen value problem. Corresponding to any value of μ there will be a discrete range of frequencies for which a wave motion with that particular propagation constant is possible.

Relation (2.25) may be rearranged to create an eigen value problem for μ, given the frequency ω. Mead [4] has demonstrated how a rearrangement of this type is possible. However for the ring under consideration, the propagation constants are obtained by a much simple procedure given by Mallik and Mead (8).

For the ring, the special type of harmonic waves propagate without any reflection as the structure does not have any ends. Hence, the ring can be considered as an infinite periodic structure except that the propagating waves should have the same phase and magnitude after travelling once around the complete ring. Consequently, frequencies (natural) at which harmonic waves can propagate are not given by the entire propagation bard but are confined to a discrete set given by

$$\mu_{rn} = 0 \ , \ \mu_{in} = \pm 2j\pi/N \ (j = 0,1,2,\ldots N) \qquad \ldots\ldots \qquad (2.26)$$

where N is the number of bays in the ring and the subscript n refers to the value at a natural frequency.

As seen from the above expression (2.26), the propagation constants always occur in pairs (positive and negative) and the number of pairs are equal to the minimum number of coupling coordinates between the adjacent periodic elements (ref. 5).

Orris and Petyt [7] have pointed out how tedious it would be, to solve a complex eigen value routine when $[K(\mu)]$ and $[M(\mu)]$ are of high order and in particular when $[M(\mu)]$ is banded rather than diagonal. Since the natural frequencies of the finite structure can be determined from the variation of the purely imaginary part of the propagation constant, it can be noted that, in assessing the modal response of the structure, the frequency variation of the imaginary propagation constant is the more important quantity. If μ is purely imaginary, the matrices in equation (2.24) and (2.25) are Hermitian. The solution of the complex eigen value problem can be reduced to that of a real symmetric matrix, as described by Wilkinson [15].

Let $$[K(\mu)] = [K^r + iK^i],\ [M(\mu)] = [M^r + iM^i] \qquad (2.27)$$

$$\{a_L^{(c)}, a_i^{(c)}\} = \{b^r + ib^i\} ;$$

Then equation 2.25 becomes

$$([K^r + iK^i] - \omega^2 [M^r + iM^i])\{ b^r + ib^i\} = 0 \qquad (2.28)$$

By separating real and imaginary parts, and combining the two sets of equations, then obtained, the matrix expression found is

$$\left(\begin{bmatrix} K^r & -K^i \\ K^i & K^r \end{bmatrix} - \omega^2 \begin{bmatrix} M^r & -M^i \\ M^i & M^r \end{bmatrix} \right) \begin{bmatrix} b^r \\ b^i \end{bmatrix} = 0 \qquad (2.29)$$

As the matrices $[K(\mu)]$, $[M(\mu)]$ are Hermitian, $K^i = -[K^i]^T$ and $[M^i] = -[M^i]^T$. Thus, equation (14) represents a real symmetric eigen value problem. The equation has been replaced by a real matrix expression, but at the expense of doubling the size of the matrices involved. The latter disadvantage is however offset by the fact that, in general more efficient computer routines are available to solve real eigen value problems.

Corresponding to each value of μ in the real matrix expression (2.29), there will be a discrete set of frequencies that occur in equal pairs. Each frequency will have associated with an eigen vector. This eigen vector defines the wave motion in periodic section at that frequency.

2.2.7 Subspace Iteration Method for Solving Eigen Value Problem:

This method is effective for finding the first few eigen values and corresponding eigen vectors of large eigen value problems whose stiffness and mass

matrices have large band widths. The various steps of this method are described briefly in Appendix B. A detailed description of the method can be found in Bathe and Wilson [10] amd several other books [11, 14, 15].

2.3 Application of the Method to Two Layered Elastic Ring With Periodic Supports:

A two layered ring, with different materials as shown in Fig. (2.1) is considered. The span between supports 1 and 2 is shown separately in Fig. (2.2). This is divided into 12 elements. Each of these elements is a 8-node isoparametric plane stress element in polar coordinates (r,θ). Radial supports are provided at the midplane radial nodes at the left and right hand boundaries as shown in Fig. (2.2).

Different support conditions are considered to get the corresponding frequencies and eigen modes, and are compared with those obtained by Reddy [9].

In the first case both the radial and tangential displacements (u and v respectively), of the supports are constrained. This results in one coupling coordinate $\frac{\partial u}{\partial \theta}$ between the two adjacent bays. Effect of increasing the rotational stiffness of the ring by including two rotational springs at the two boundaries is also considered.

In the second case, only the radial displacement 'u' is constrained at both the supports. This results in two coupling coordinates v, $\frac{\partial u}{\partial \theta}$ between the adjacent bays. Since there exists a rigid body rotation in this case, the method described by Zienkiwicz [13] is used to overcome the problem of singular stiffness matrix. This method primarily involves shifting the frequencies by an amount α, and subtracting the same after solving the eigen value expression.

For all the cases considered above, mode shapes have been plotted.

2.4 Application of the Method to Three Layered Orthotropic Ring with Periodic Supports:

A three layered ring as shown in Fig. (2.3) has been considered for the present work, with outer and inner layers having the fibre orientation as shown in Fig. (2.6) and the middle layer having the fibre orientation as shown in Fig. (2.7).

One bay of the three layered ring with three supports is considered for obtaining the natural frequencies and mode shapes using 'wave approach'. Each one of the layers, in the 3 layered bay, is divided into six 8-node isoparametric elements, totalling upto 18 elements. Since each of the outer and inner layers

has different fibre orientation, it is interesting to see how the three layered ring behaves when a free wave propagates. Frequencies and mode shapes are obtained for monocoupling case where both radial and tangential displacements of the nodes situated on the midplane radius of layer three are constrained giving rise to only one coupling coordinate $\frac{\partial u}{\partial \varphi}$.

CHAPTER - III

RESULTS AND DISCUSSION

3.1 Introduction

The accuracy with which the propagation constants and their corresponding natural frequencies can be obtained by finite element method is first checked by comparing the results for periodically supported beam against the results of [7] and other workers. Next the results are compared for two cases of a periodically supported two layered elastic ring with those obtained by [9]. Finally, frequencies and mode shapes of a three layered orthotropic ring obtained by the present method are shown.

3.2 Frequencies for Periodically Supported Beams Ref. to a Fig. (3.5a) of Beam:

To check the accuracy of the developed FEM computer program, the purely imaginary part of the propagation constant is plotted as a function of non-dimensional frequency. The curve Figure (3.5b) is found to be exactly matching with that presented in earlier work. Petyt's results need correction by a factor of 40.

3.3 Two-Layered Elastic Ring on Three Periodic Supports:

The present finite element analysis is used to obtain the natural frequencies and mode shapes of two layered elastic ring on three periodic radial supports as shown in Fig. (2.1). The numerical data presented by Reddy [9] is considered here for better comparison of results. This is presented as follows:

$$\delta_2 = 0.02, \quad E_1/E_2 = 0.001 , \quad \rho_1/\rho_2 = 0.2$$

$$N = 3 \text{ (three supports)}, \quad \bar{K}_r = 0 \text{ and } 2.$$

where $\delta_2 (= h_2/R_2)$ is the ratio of half thickness to midplane radius of layer 2 , E_1 and E_2 are Young's modulii of elasticity for outer and inner layers, ρ_1 and ρ_2 are mass densities corresponding to layer 1 and layer 2, $N = 3$ (number of supports of the ring), $\bar{K}_r$ is a nondimensional rotational stiffness applied in the form of spring at both the boundaries of one bay of the ring.

3.3.1 Monocoupled Two Layer Ring on Three Supports with $\bar{K}_r = 0$

The nondimensional natural frequencies obtained are tabulated in Table 3.1 along with those obtained by Reddy [9] for the phase constants $\mu = 0, 2\pi/3$, where the nondimensional natural frequency is given by

$$\Lambda_n = \sqrt{m_2/D_2}$$

where m_2 is mass of the base layer 2 over a length of R_i.

$= 2\ t\ h_2\ \rho_2\ R_2$

where δ_2 is density of material of base layer 2

b is width of the ring

D_2 is the bending stiffness

$= \frac{2}{3}\ E_2\ b\ \delta_2^3$

where $\delta_2 = h_2/R_2$

h_2 is bay thickness of base layer 2

E_2 is Young's modulus elasticity of base layer 2

R_2 is radius of the ring.

From the Table 3.1 it can be observed that the error by the present analysis is within 0.5% of those presented by Ref. [9]. Also for the positive going wave ($\mu_{in} = -2\pi/3$) and negative going wave ($\mu_{in} = +2\pi/3$) the frequencies are found to be exactly matching. The number of subspace iteration vectors used to obtain first four frequencies accurately are 8 and this has taken 16 iterations to converge. The computer processing time is noted to be 480 sec. (computer time) mode shapes:

The eigen value expression (Eq. 2.29) derived in sec. 2.2.5, gives complex eigen vectors $\begin{Bmatrix} b^r \\ b^i \end{Bmatrix}\begin{Bmatrix} b^i \\ b^r \end{Bmatrix}$

for the same frequency for a given value of phase constant. This is because of the doubling the size of the eigen value expression given by Eq. 2.25. We consider only $\{ \begin{matrix} b^r \\ b^i \end{matrix} \}$ as this is the vector required by expression 2.25. For $\mu_{in} = + 2\pi/3$ and $\mu_{in} = - 2\pi/3$ also, vectors $\{ \begin{matrix} b^{r+} \\ b^{i+} \end{matrix} \}$ and $\{ \begin{matrix} b^{r-} \\ b^{i-} \end{matrix} \}$ are obtained (Table 3.5).

It is observed from the results obtained that, in the present analysis, the eigen value , at $\mu_{in} = +2\pi/3$ and $\mu_{in} = -2\pi/3$, is not repeated. But it has been established Ref. [8] that there are degeneracies at these frequencies.

In the work by Reddy [9], it is noted that for a standing mode to exist at a natural frequency the moments M^+ and M^- of the positive going wave and negative going at both the supports should be either in phase or anti phase with each other. This is earlier been verified experimentally also by Mallik and Mead [8]. Since there are two conditions at which the mode can exist at $\mu_{in} \neq 0$, stated as above, there is bound to be a degeneracy of modes at the frequencies at which $\mu_{in} \neq 0$.

The present finite element analysis does not directly lead us to the second eigen vector at these degenerate frequencies. Rather knowing that a second eigen vector at the same frequency for $\mu_{in} \neq 0$ may exist,

and also that the standing waves are sought for, an explanation for the existence of second eigen vector is given in the following.

The total deflection vector will be a sum of positive and negative going waves for the first bay of the ring, given by $\{b\} = \{\{b^{r+}\} + i\{b^{i+}\}\} + \{\{b^{r-}\} + i\{b^{i-}\}\}$, where $\{b^{r+}\}$ is real part of $\mu_{in} = -2\pi/3$ and $\{b^{i+}\}$ is the imaginary part of the positive going wave and $\{b^{r-}\}$ and $\{b^{r}\}$ are the real and imaginary parts of negative going wave at $\mu_{in} = +2\pi/3$. For standing waves to exist, the phase difference between positive going wave and negative going wave has to be zero leading to either $\{b^{i+}\} = -\{b^{i-}\}$ or $\{b^{r+}\} = -\{b^{r-}\}$.

Since the results presented in Table 3.5 show that $\{\{b^{r+}\} + i\{b^{i+}\}\}$ is not the complex conjugate of either $\{\{b^{r-}\} + i\{b^{i-}\}\}$ or $-\{\{b^{r-}\} + i\{b^{i-}\}\}$. It is guessed that at $\mu_{in} = 2\pi/3$, there is another eigenvector $\{\{b^{r+}\} - i\{b^{i+}\}\}$ and similarly at $\mu_{in} = -2\pi/3$ there is another eigen vector equal to $\{\{b^{r-}\} - i\{b^{i-}\}\}$. With this expectation, the standing wave at $\mu = -2\pi/3$ is given by $\{b^{r+}\}$ and at $\mu = +2\pi/3$ by $\{b^{-r}\}$. The results are plotted in Fig. (3.1) for each bay of the ring and these are found to be matching with shapes presented by Reddy [9]. This supports the explanation given above.

TABLE 3.1

Natural frequencies of two layered elastic ring with monocoupling and $\bar{K}_r = 0$

$\rho_1/\rho_2 = 0.2$, $E_1/E_2 = 0.001$, $\delta_2 = 0.02$

$\delta_1/\delta_2 = 2$, N = 3 (Number of supports)

Mode No.	μ_{in}	Ω_n	
		Finite element results	Ref. (9) results
1	0	5.959	5.973
2	$+2\pi/3$	8.947	8.976
3	$+2\pi/3$	16.412	16.381
4	0	20.210	20.13

TABLE 3.2

Natural frequencies of two layered elastic ring with monocoupling and $\bar{K}_r = 2$

$\rho_1/\rho_2 = 0.2$, $E_1/E_2 = 0.001$, $\delta_2 = 0.02$

$\delta_1/\delta_2 = 2$, $N = 3$ (Number of supports)

Mode No.	μ_{in}	Ω_n	
		Finite element results	Ref. (9) results
1	0	6.602	6.619
2	$+2\pi/3$	9.148	9.179
3	$+2\pi/3$	16.788	16.750
4	0	20.21	20.13

TABLE 3.3

Natural frequencies of two layered elastic ring with Bicoupling and $\bar{K}_r = 0$

$\rho_1/\rho_2 = 0.2$, $E_1/E_2 = 0.001$, $\delta_2 = 0.02$

$\delta_1/\delta_2 = 2$, N = 3 (Number of supports)

Mode No.	μ_{in}	Ω_n	
		Finite element results	Ref.(9) Results
1	0	0.1	0.0
2	+ 2π/3	1.416	1.414
3	0	6.570	6.581
4	+ 2π/3	9.002	9.031

TABLE 3.4

Natural frequencies of three layered orthotropic ring with monocoupling and $\bar{K}_r = 0$ (same material for all 3 layers)

$\delta_3 = 0.015$, $\delta_2/\delta_3 = 2$, $\delta_1/\delta_3 = 1$, N = 3 (Number of supports)

Mode No.	μ_{in}	Ω_n Finite element results
1	0	23.986
2	+ 2π/3	37.668
3	+ 2π/3	59.971
4	0	74.031

TABLE 3.5

DISPLACEMENT VECTORS FOR THE TWO LAYERED RING WITH MONOCOUPLING AND $\bar{K}_r = 0$

Case (i) $\mu_{in} = 0$ Frequency: ω_n 5.959

Node No.	First Bay	Second Bay	Third Bay
2	0.0	0.0	0.0
10	-0.4	-0.4	-0.4
18	-0.4	-0.4	-0.4
26	0.0	0.0	0.0
34	0.4	0.4	0.4
42	0.4	0.4	0.4
50	0.0	0.0	0.0

Case (ii) $\mu_{in} = 2\pi/3$ Frequency: ω_n 8.947

2	0.0	0.0	0.0
10	-0.09	-0.61	0.71
18	-0.45	-0.48	0.93
26	-0.28	0.24	0.03
34	0.26	0.64	-0.91
42	0.47	0.28	-0.76
50	0.0	0.0	0.0

Case (iii) $\mu_{in} = +2\pi/3$ Frequency: ω_n 8.947

2	0.0	0.0	0.0
10	-0.49	-0.26	0.75
18	-0.82	+0.02	0.80
26	-0.17	+0.30	-0.12
34	0.71	+0.17	-0.88
42	0.72	-0.14	-0.58
50	0.0	0.0	0.0

TABLE 3.6

DISPLACEMENT VECTORS FOR THE TWO LAYERED RING WITH MONOCOUPLING AND $\bar{\bar{K}}_r = 2$

Case (i) $\mu_{in} = 0$, Frequency $\Omega_n = 6.602$

Node No.	First Bay	Second Bay	Third Bay
2	0.0	0.0	0.0
10	0.84	0.84	0.84
18	0.87	0.87	0.87
26	0.0	0.0	0.0
34	-0.87	-0.87	-0.87
42	-0.84	-0.84	-0.84
50	0.0	0.0	0.0

Case (ii) $\mu_{in} = + 2\pi/3$ Frequency $\Omega_n = 9.148$

2	0.0	0.0	0.0
10	-0.50	0.74	-0.24
18	-0.38	0.95	-0.57
26	+0.23	0.00	-0.22
34	+0.52	-0.95	+0.43
42	+0.20	-0.73	0.54
50	0.0	0.0	0.0

Case (iii) $\mu_{in} = - 2\pi/3$ Frequency $\Omega_n = 9.148$

2	0.0	0.0	0.0
10	-0.07	0.69	-0.62
18	0.22	0.69	-0.90
26	0.26	-0.16	-0.09
34	-0.05	-0.80	0.85
42	-0.27	-0.50	0.75
50	0.0	0.0	0.0

TABLE 3.7

DISPLACEMENT VECTORS FOR THE TWO LAYERED RING WITH BI-COUPLING AND $\bar{K}_r = 0$

Case (i) $\mu_{in} = 0$ Frequency ω_n = 6.57

Node No.	First Bay	Second Bay	Third Bay
2	0.0	0.0	0.0
10	-0.92	-0.92	-0.92
18	-0.92	-0.92	-0.92
26	0.0	0.0	0.0
34	0.92	0.92	0.92
42	0.92	0.92	0.92
50	0.0	0.0	0.0

Case (ii) $\mu_{in} = +2\pi/3$ Frequency ω_n = 1.41

2	0.0	0.0	0.0
10	-0.26	-0.16	0.43
18	-0.35	-0.41	0.76
26	-0.29	-0.57	0.37
34	-0.14	-0.57	0.72
42	-0.12	-0.37	0.38
50	0.0	0.0	0.0

Case (iii) $\mu_{in} = -2\pi/3$ Frequency ω_n = 1.41

2	0.0	0.0	0.0
10	0.26	-0.16	+0.43
18	0.36	-0.30	+0.76
26	0.30	-0.57	-0.002
34	0.15	-0.57	-0.72
42	0.01	-0.36	-0.38
50	0.0	0.0	0.0

TABLE 3.8

DISPLACEMENT VECTORS FOR THE THREE LAYERED ORTHOTROPIC RING WITH MONOCOUPLING AND $\bar{\bar{K}}_r = 0$

Case (i) $\mu_{in} = 0$ Frequency $\bar{\omega}_n$ = 23.98

Node No.	First Bay	Second Bay	Third Bay
2	0.0	0.0	0.0
13	0.37	0.37	0.37
24	0.36	0.36	0.36
35	0.0	0.0	0.0
46	-0.36	-0.36	-0.36
57	-0.37	-0.37	-0.37
68	0.0	0.0	0.0
	Case (ii) $\mu_{in} = +2\pi/3$	Frequency $\bar{\omega}_n$ = 37.66	
2	0.0	0.0	0.0
13	0.31	0.34	0.03
24	0.22	0.47	0.25
35	-0.18	0.10	0.23
46	-0.40	0.35	-0.02
57	-0.18	0.38	-0.19
68	0.0	0.0	0.0
	Case (iii) $\mu_{in} = -2\pi/3$	Frequency $\bar{\omega}_n$ = 37.66	
2	0.0	0.0	0.0
13	0.36	-0.08	-0.25
24	0.46	-0.2	-0.15
35	0.15	-0.25	0.20
46	-0.4	+0.1	0.35
57	-0.4	0.24	0.13
68	0.0	0.0	0.0

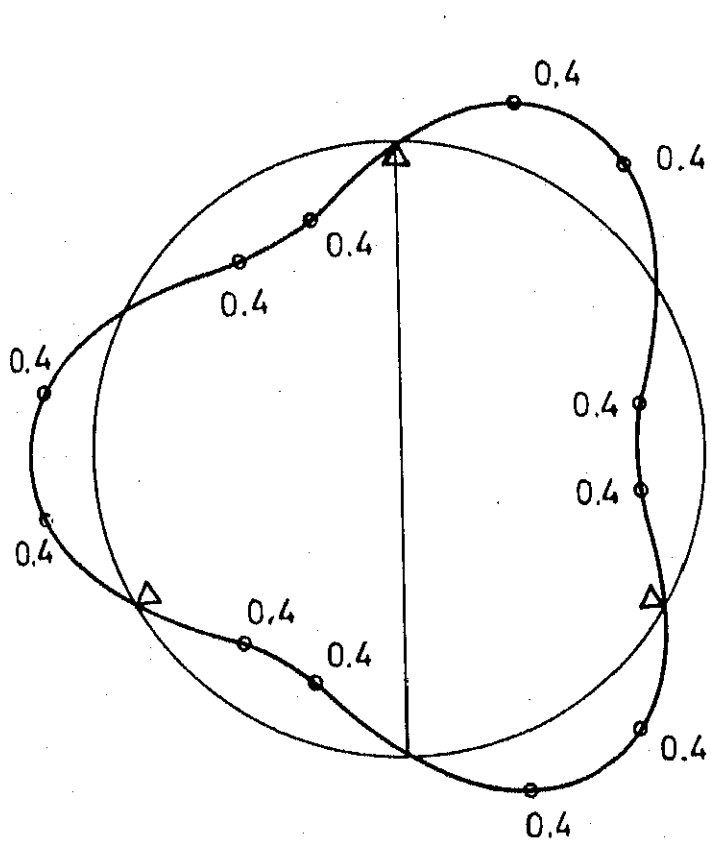

MODE 1
$\Omega_n = 5.959$
$\mu_{in} = 0$

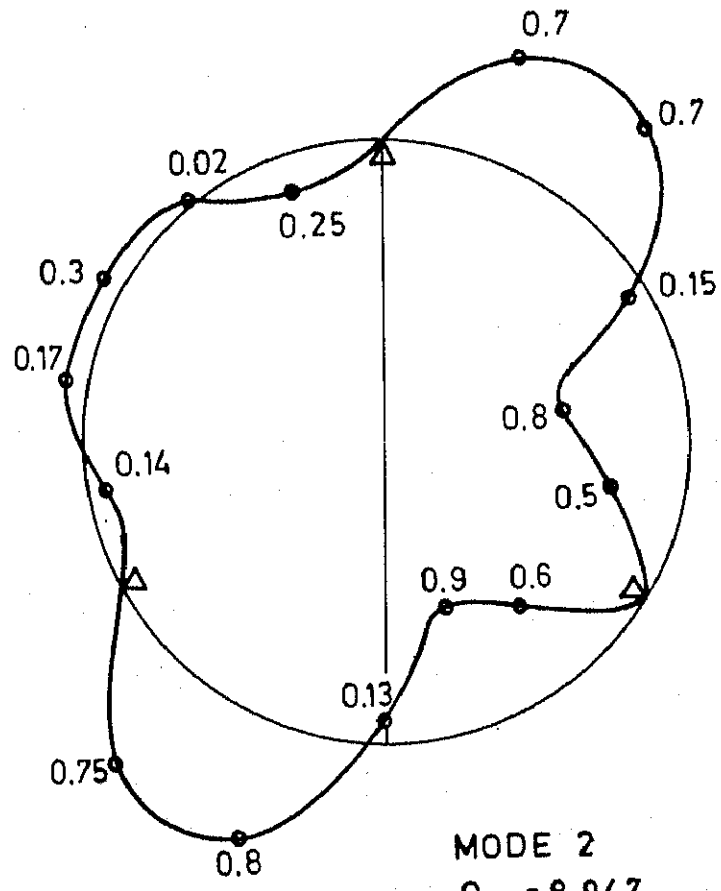

MODE 2
$\Omega_n = 8.947$
$\mu_{in} = +2\pi/3$ Symm

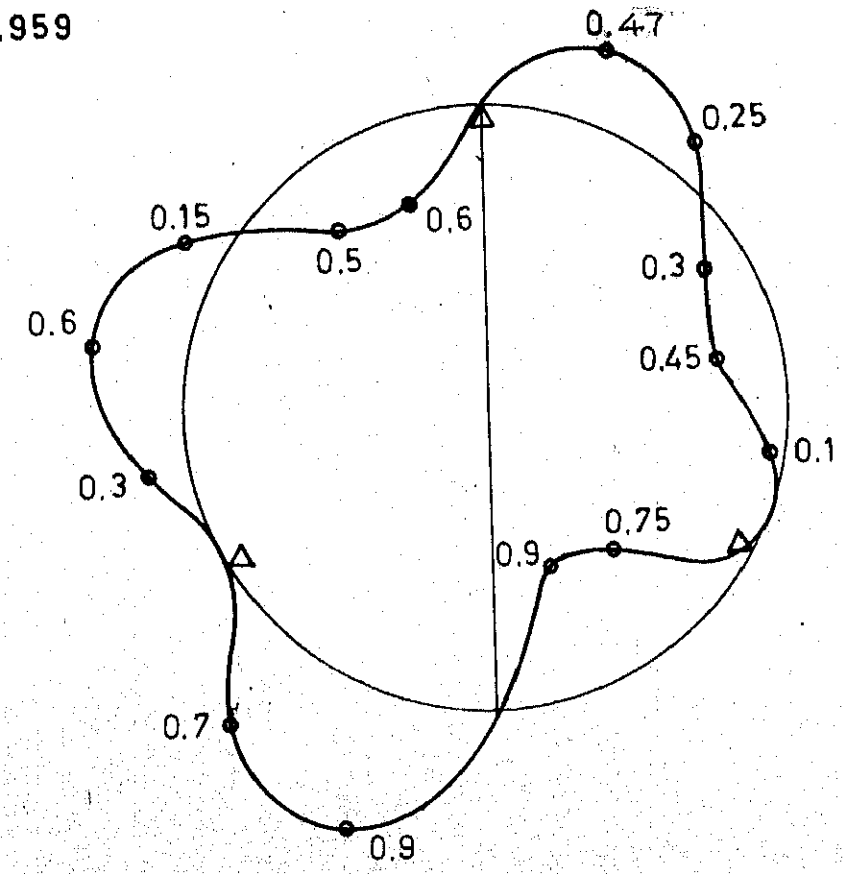

MODE 3
$\Omega_n = 8.947$
$\mu_{in} = -2\pi/3$ Anti Symm

FIG. 3.1 MODE SHAPES (U) OF TWO LAYERED RING MONO COUPLED SYSTEM, $\bar{K}_r = 0$

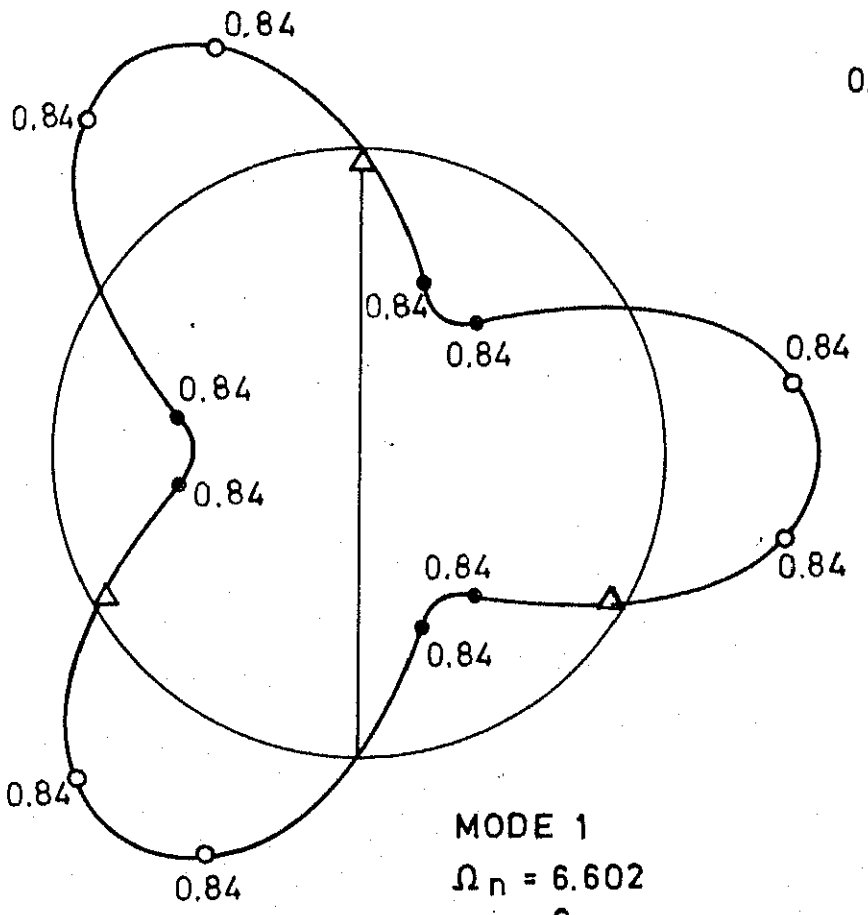

MODE 1
Ω_n = 6.602
μ_{in} = 0

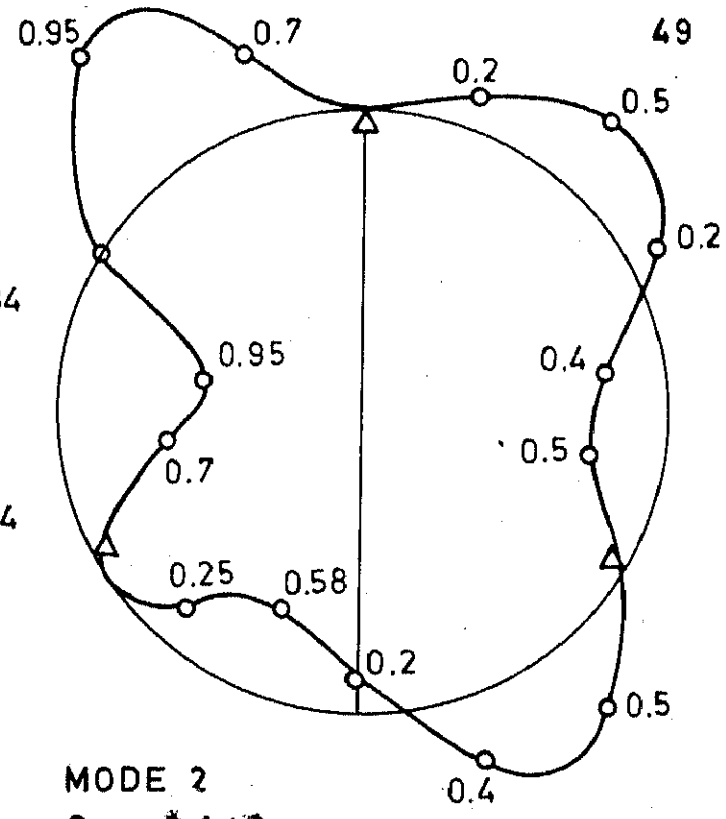

MODE 2
Ω_n = 9.148
μ_{in} = $+2\pi/3$ Anti-Symm.

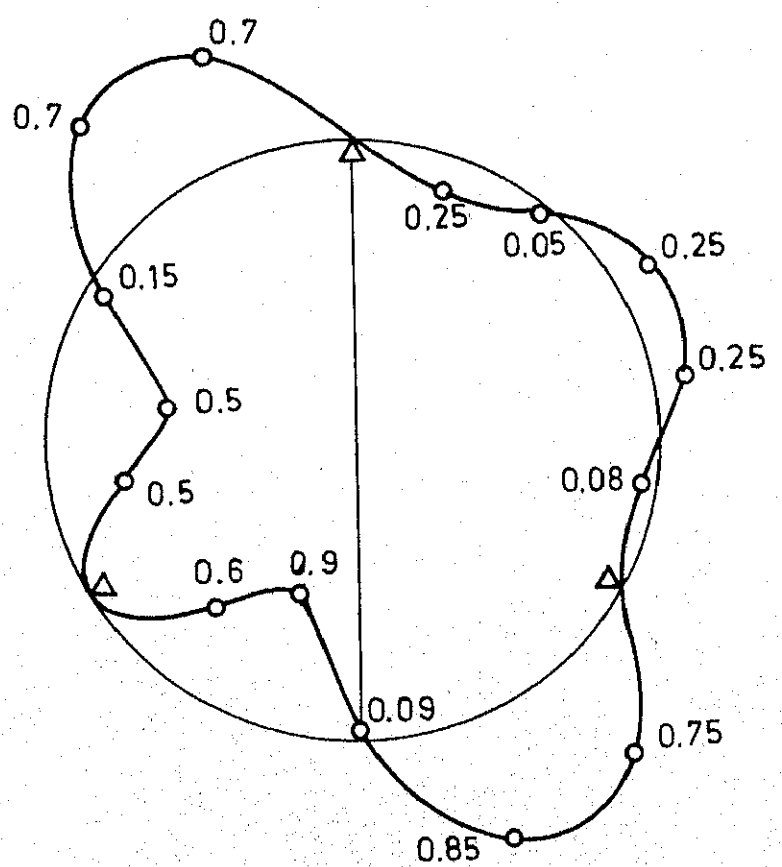

MODE 3
Ω_n = 9.148
μ_{in} = $-2\pi/3$ Symm.

FIG. 3.2 MODE SHAPES (U) OF TWO LAYERED RING MONO COUPLED SYSTEM, $\bar{K}_r = 2$

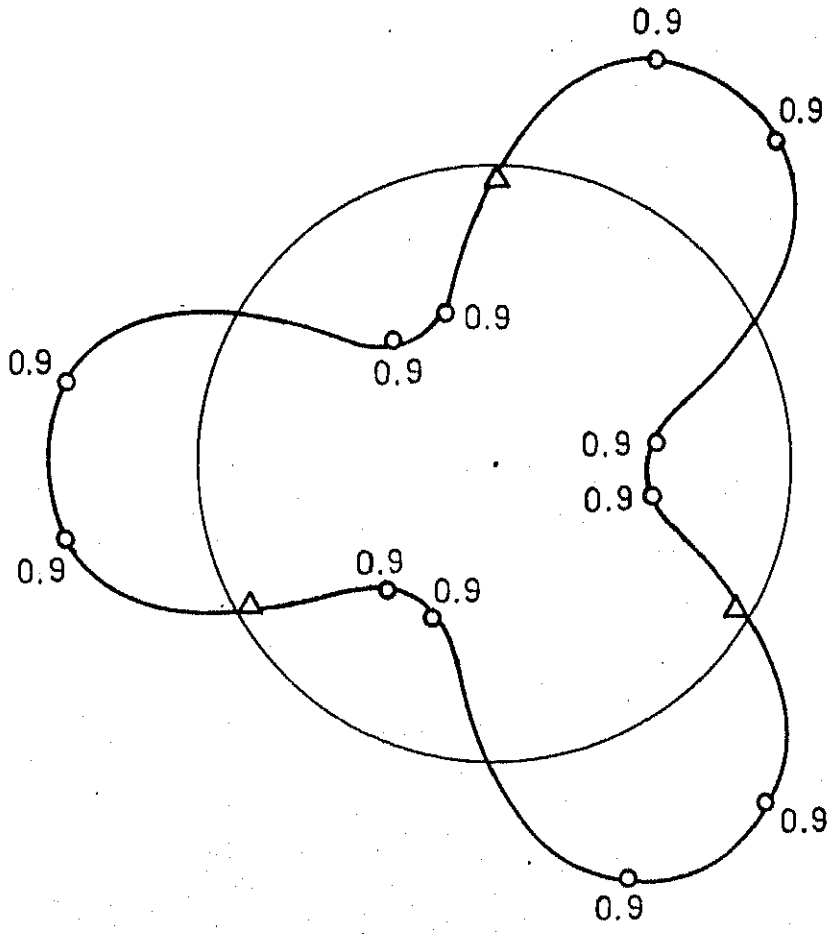

MODE 1
Ω_n = 6.57
μ_{in} = 0

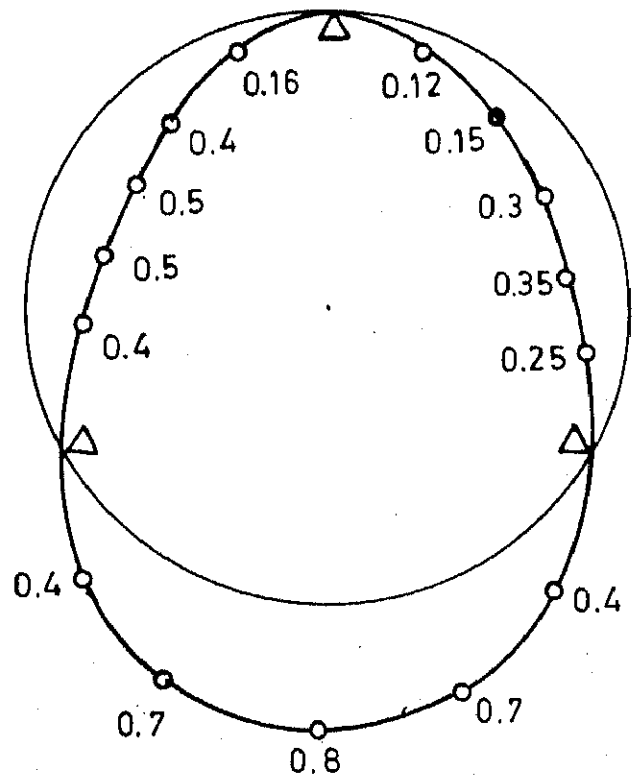

MODE 2
Ω_n = 1.41
μ_{in} = ± 2π/3 Symm.

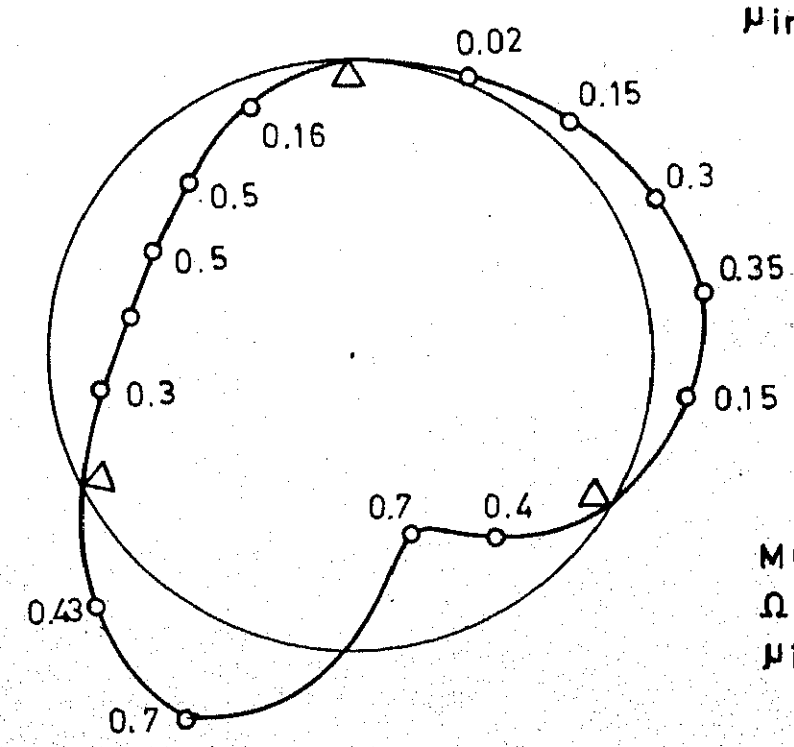

MODE 3
Ω_n = 1.41
μ_{in} = −2π/3
Anti Symm

FIG. 3.3 MODE SHAPES (U) OF TWO LAYERED RING BICOUPLED SYSTEM, $\bar{K}_r = 0$

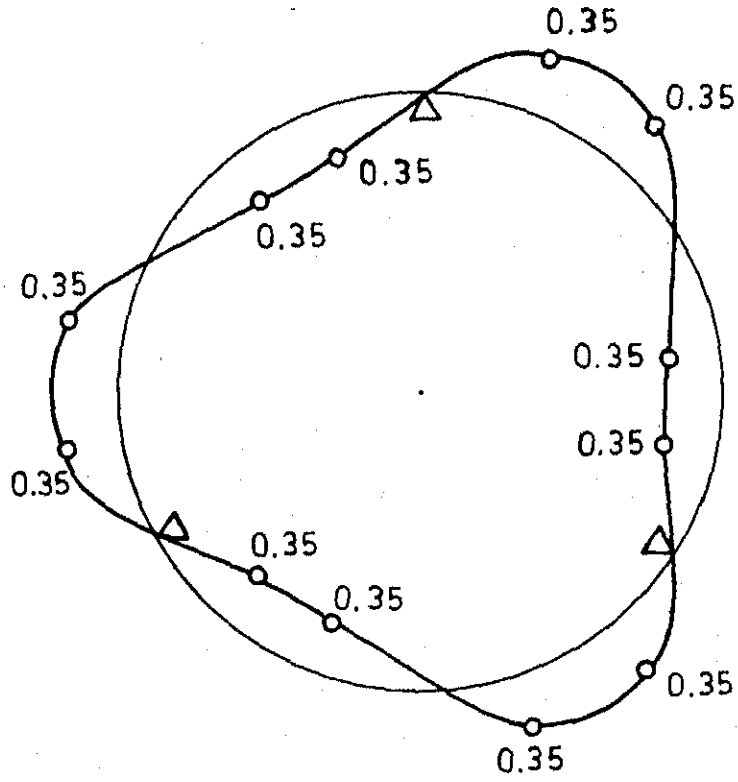

MODE 1
$\Omega_n = 23.98$
$\mu_{in} = 0$

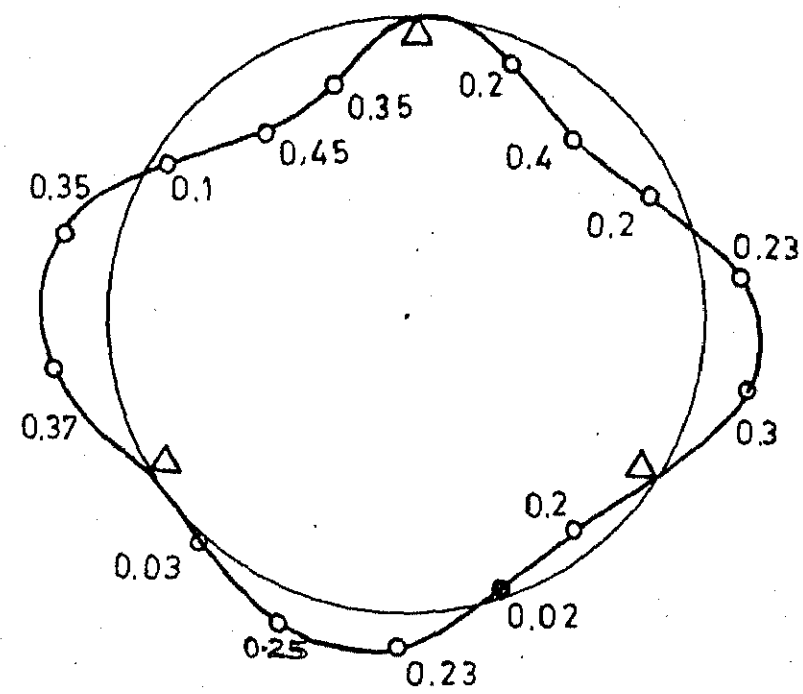

MODE 2
$\Omega_n = 37.66$
$\mu_{in} = +2\pi/3$

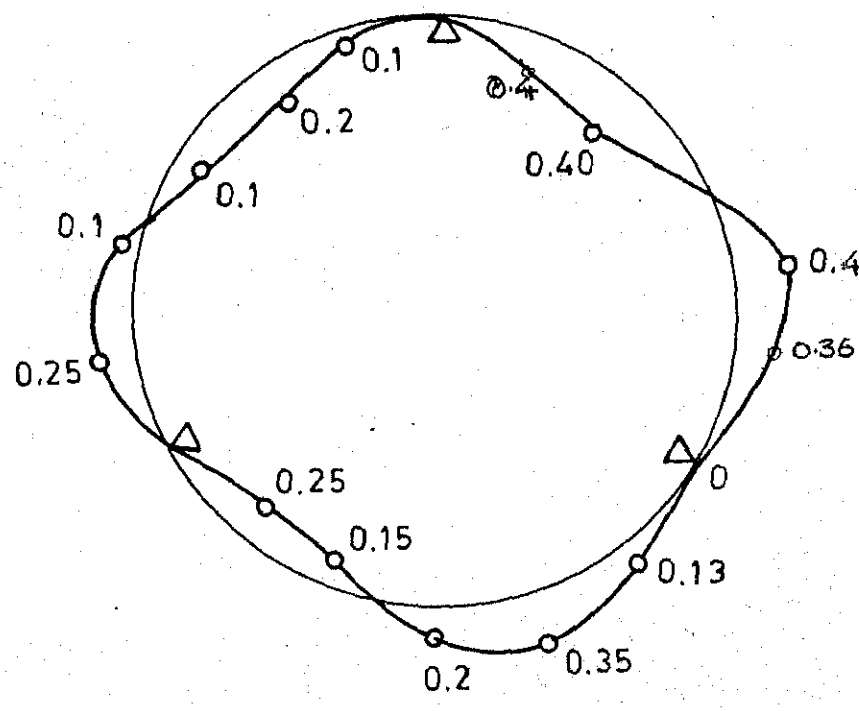

MODE 3
$\Omega_n = 37.66$
$\mu_{in} = -2\pi/3$

FIG. 3.4 MODE SHAPES (U) OF THREE LAYERED ORTHOTROPIC RING MONOCOUPLED SYSTEM, $\overline{K}_r = 0$

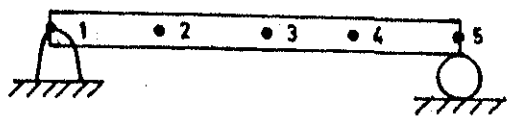

FIG. 3.5(a) ONE BAY OF A PERIODICALLY SUPPORTED BEAM ON SIMPLE SUPPORTS.

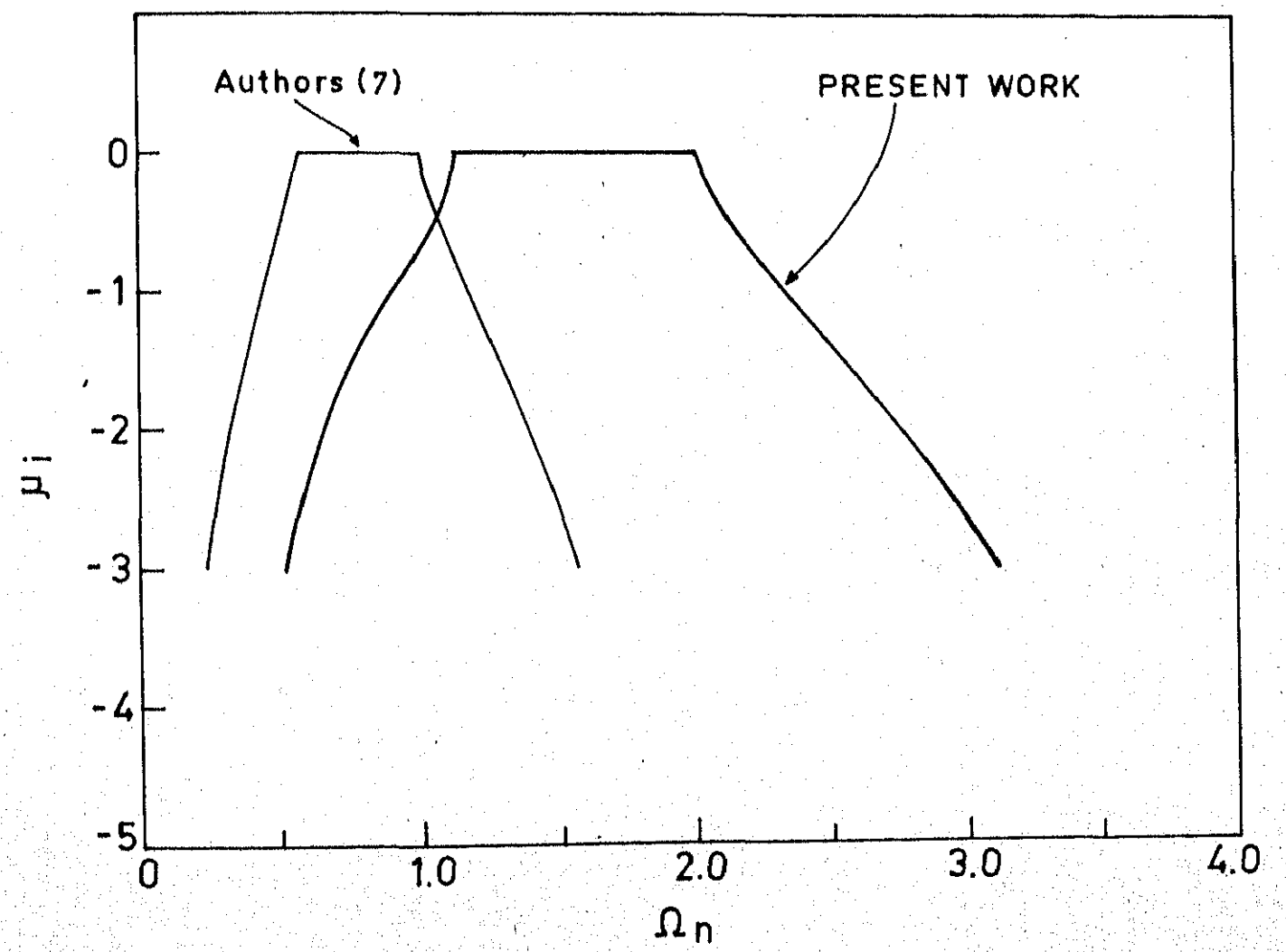

FIG. 3.5(b) VARIATION OF IMAGINARY PART OF PROPAGATION CONSTANT AND NONDIMENSIONAL FREQUENCY.

3.3.2 Monocoupled Two Layer Ring on Three Supports with $\bar{K}_r = 2$:

The rotation stiffness is included in this case by means of springs at the two boundaries. The natural frequencies for this case are tabulated in Table 3.2. And the Table 3.6 shows the displacement vectors for the three bays of the ring. The mode shapes are plotted as shown in Fig. 3.2 and these are found to be matching well with those obtained by Reddy [9].

The frequencies in this case also are found to be with 0.5% accuracy compared to (Ref. 9). The initial eigen vector taken for first 4 frequencies to converge are eight, and the CPU time in this case also is found to be 480 sec. for a total of 15 subspace iterations.

3.3.3 Bi-Coupled Two Layer Ring on 3 Supports with $\bar{K}_r=0$

The boundary conditions in this case are to constrain radial degree of freedom at nodes 2 and 50 as shown in Fig. 2.2. Here there is a rigid body rotation. So the first frequency obtained should be zero. The rigid body mode is suppressed as explained in Section 2.3

The natural frequencies are tabulated in Table 3.3 and the Table 3.7 shows the displacement vectors for

the three bays of the ring. From Table 3.3 it is observed that due to numerical error, the frequency for rigid body mode is shown as 0.1. All the frequencies are found to be within 0.5% accuracy compared to those in (Ref.9). The number of initial eigen vectors chosen in this case are 8 to obtain first 4 frequencies accurately and this has taken 439 sec. of CPU time for 16 iterations of convergence. The mode shapes plotted are as shown in Fig. 3.3 and these also match well with those obtained by Reddy [9].

3.5 Conclusion:

Many researchers have found exact harmonic solutions for finding propagation constants and frequencies in the case of periodically supported structures, when the material is isotropic. It becomes difficult to get harmonic solutions for complex problems analytically when the material is anisotropic. The finite element method presented in this work has revealed that the material orthotropy can easily be included in the analysis to find natural frequencies and corresponding mode shapes.

REFERENCES

1. L. Brillouin 1946 wave propagation in periodic structures New York : Dover Publication, Inc.

2. M.A. Heckl 1964 Journal of the Acoustical Society of America 36, 1335-1343. Investigations on the vibrations of grillages and other simple beam structures.

3. D.J. Mead 1966 shock and vibration bulletin 35, 45-54. The random vibrations of a multi-supported heavily damped beam.

4. D.J. Mead 1970 Journal of Sound and vibration 11, 181-197. Free wave propagation in periodically supported infinite beams.

5. D.J. Mead 1973 Journal of Sound and vibration 27, 235-260. A general theory of harmonic wave propagation in linear periodic systems with multiple coupling.

6. A.L. Abrahamson 1973. Journal of sound and vibration 28, 247-258. Flexural wave mechanics - an analytical approach to vibration of periodic structures forced by convected pressure fields.

7. Ruth M. Orris and M. Petyt 1974 Journal of Sound and vibration 33(2), 223-236. A finite element study of harmonic wave propagation in periodic structure.

8. Mallik A.K. and D.J. Mead 1977. Journal of Sound and vibration 54, 13-27, Free vibration of thin circular rings on periodic radial supports.

9. E.S. Reddy, 1982, Ph. D. Thesis, IIT Kanpur, 'In-plane vibrations of layered rings on periodic radial supports'.

10. K.L. Bathe and E.L. Wilson : Large eigen value problems in dynamic analysis.

11. S.S. Rao The finite element method in engineering, Pargamon Press, New York.

12. Bathe and Wilson Numerical methods in finite element analysis.

13. Zienkiewicz, The finite element method.

14. Bathe, Oden, Wunderlich, 1977 Formulation and computational algorithms in finite element analysis US. - Germany Symposium MIT, USA.

15. Wilkinson, 1976. The algebraic eigen value problem. Oxford: The Clerendon Press.

APPENDIX A

SHAPE FUNCTIONS OF 8-NODE ISOPARAMETRIC ELEMENT

$$N_1 = \frac{1}{4}(1-s)(1-t_1) - (\frac{1}{2})N_5 - (\frac{1}{2})N_8$$

$$N_2 = \frac{1}{4}(1-s)(1-t_1) - (\frac{1}{2})N_5 - (\frac{1}{2})N_6$$

$$N_3 = \frac{1}{4}(1-s)(1+t_1) - (\frac{1}{2})N_6 - (\frac{1}{2})N_7$$

$$N_4 = \frac{1}{4}(1-s)(1+t_1) - (\frac{1}{2})N_7 - (\frac{1}{2})N_8$$

$$N_5 = \frac{1}{2}(1-s^2)(1-t_1)$$

$$N_6 = \frac{1}{2}(1-t_1^2)(1+s)$$

$$N_7 = \frac{1}{2}(1-s^2)(1+t_1)$$

$$N_8 = \frac{1}{2}(1-t_1^2)(1-s)$$

APPENDIX B

RAYLEIGH-RITZ

SUBSPACE ITERATION METHOD

This method of solving eigen value express of the form

$$\{[A] - \omega^2 [B]\} \{X\} = 0$$

where [A] and [B] are real symmetric consists of the following steps.

Step 1 : Start with q initial iteration vectors $X_1, X_2, \ldots X_q$, $q > p$, where p is the number of eigen values and eigen vectors to be calculated. Bathe and Wilson suggested e value of $q = \min(2p, p+8)$ for good convergence. Define the initial modal matrix $[X_o]$ as

$$[X_o] = [\vec{X}_1 \; \vec{X}_2 \ldots \vec{X}_q]$$

and set the iteration number $k = 0$.

Step 2 : The following subspace iteration procedure is used to generate an improved modal matrix $[X_{k+1}]$:

(a) Find $[\bar{X}_{k+1}]$ from the relation

$$[A] [\bar{X}_{k+1}] = [B] [X_k]$$

(b) Compute

$$[A_{k+1}] = [\bar{X}_{k+1}]^T [A] [\bar{X}_{k+1}] \text{ and}$$

$$[B_{k+1}] = [\bar{X}_{k+1}]^T [B] [\bar{X}_{k+1}]$$

(c) Solve for the eigen values and eigen vectors of the reduced system

$$[A_{k+1}] [Q_{k+1}] = [B_{k+1}] [Q_{k+1}] [\Lambda_{k+1}]$$

and obtain $[\Lambda_{k+1}]$ and $[Q_{k+1}]$

(d) Find an improved approximation to the eigen vectors of the original system as

$$[X_{k+1}] = [\bar{X}_{k+1}] [Q_{k+1}]$$

Step 3: If $\lambda_i^{(k)}$ and $\lambda_i^{(k+1)}$ denote the approximations to the i^{th} eigen value in the iteration k-1 and k respectively, we assume convergence of the process whenever the following criteria are satisfied:

$$\left| \frac{\lambda_i^{(k+1)} - \lambda_i^{(k)}}{\lambda_i^{(k+1)}} \right| \leq \text{eps}, \quad i = 1,2,\ldots p$$

where eps = 10^{-6}. It is to be noted that although the iteration is performed with q vectors ($q > p$), the convergence is measured only on the approximations predicted for the p smallest eigen values.